Neocortical Neuronal Morphology in the Newborn Giraffe (*Giraffa camelopardalis tippelskirchi*) and African Elephant (*Loxodonta africana*)

Bob Jacobs,[1]* Laura Lee,[1] Matthew Schall,[1] Mary Ann Raghanti,[2] Albert H. Lewandowski,[3] Jack J. Kottwitz,[4] John F. Roberts,[5] Patrick R. Hof,[6] and Chet C. Sherwood[7]

[1]Laboratory of Quantitative Neuromorphology, Department of Psychology, Colorado College, Colorado Springs, Colorado 80903
[2]Department of Anthropology, Kent State University, Kent, Ohio 44242
[3]Cleveland Metroparks Zoo, Cleveland, Ohio 44109
[4]Department of Anatomy, Physiology, and Pharmacology, College of Veterinary Medicine, Auburn University, Auburn, Alabama 36849
[5]Thompson Bishop Sparks State Diagnostic Laboratory, Alabama Department of Agriculture and Industries, Auburn, Alabama 36849
[6]Fishberg Department of Neuroscience and Friedman Brain Institute, Icahn School of Medicine at Mount Sinai, New York, New York 10029
[7]Department of Anthropology, The George Washington University, Washington, DC 20052

ABSTRACT

Although neocortical neuronal morphology has been documented in the adult giraffe (*Giraffa camelopardalis tippelskirchi*) and African elephant (*Loxodonta africana*), no research has explored the cortical architecture in newborns of these species. To this end, the current study examined the morphology of neurons from several cortical areas in the newborn giraffe and elephant. After cortical neurons were stained with a modified Golgi technique (N = 153), dendritic branching and spine distributions were analyzed by using computer-assisted morphometry. The results showed that newborn elephant neurons were considerably larger in terms of all dendritic and spine measures than newborn giraffe neurons. Qualitatively, neurons in the newborns appeared morphologically comparable to those in their adult counterparts. Neurons in the newborn elephant differed considerably from those observed in other placental mammals, including the giraffe, particularly with regard to the morphology of spiny projection neurons. Projection neurons were observed in both species, with a much larger variety in the elephant (e.g., flattened pyramidal, nonpyramidal multipolar, and inverted pyramidal neurons). Although local circuit neurons (i.e., interneurons, neurogliaform, Cajal–Retzius neurons) resembled those observed in other eutherian mammals, these were usually spiny, which contrasts with their adult, aspiny equivalents. Newborn projection neurons were smaller than the adult equivalents in both species, but newborn interneurons were approximately the same size as their adult counterparts. Cortical neuromorphology in the newborn giraffe is thus generally consistent with what has been observed in other cetartiodactyls, whereas newborn and adult elephant morphology appears to deviate substantially from what is commonly observed in other placental mammals. J. Comp. Neurol. 000:000–000, 2015.

INDEXING TERMS: dendrite; morphometry; Golgi method; brain evolution; neocortex; nif-0000–10294

Recent investigations into the morphology of neocortical neurons in relatively large brained mammals have revealed evolutionarily conserved features across species, but also some characteristics that are unique within phylogenetic groups. Within cetartiodactyls, pyramidal neurons are the dominant type in the neocortex, with an apical dendrite morphology that appears to exist along a continuum from those that are similar to apical dendrites in "typical" (i.e., primate/rodent-like)

Grant sponsor: The James S. McDonnell Foundation; Grant numbers: 22002078 (to P.R.H. and C.C.S.); 220020293 (to C.C.S).

*CORRESPONDENCE TO: Bob Jacobs, Ph.D., Laboratory of Quantitative Neuromorphology, Department of Psychology, Colorado College, 14 E. Cache La Poudre, Colorado Springs, CO 80903.
E-mail: BJacobs@ColoradoCollege.edu

Received April 28, 2015; Revised June 19, 2015;
Accepted June 22, 2015.
DOI 10.1002/cne.23841
Published online Month 00, 2015 in Wiley Online Library (wileyonlinelibrary.com)

pyramidal neurons (Bianchi et al., 2012) to those that differ slightly in terms of apical branching profiles (e.g., humpback whale, minke whale, bottlenose dolphin: Butti et al., 2015; pygmy hippopotamus: Butti et al., 2014; giraffe: Jacobs et al., 2015). In the African elephant neocortex, however, neuronal morphology is distinct from all other placental mammals examined to date (Jacobs et al., 2011), including other afrotherians like the rock hyrax (Bianchi et al., 2011). Specifically, differences in the elephant projection neurons are manifested not only in apical dendrite morphology, which is characterized by widely bifurcating rather than singularly ascending apical dendrites (Mountcastle, 1997; Innocenti and Vercelli, 2010), but also by the prevalence of several horizontally oriented spiny neurons such as flattened pyramidal and nonpyramidal multipolar neurons (Jacobs et al., 2011). The neuronal morphology observed in these species to date, however, has been limited to the adult neocortex. The present study addresses this deficit by exploring the neuronal morphology in several neocortical regions of the newborn giraffe (*Giraffa camelopardalis tippelskirchi*) and African elephant (*Loxodonta africana*). The availability of well-preserved newborn brain tissue in both the elephant and giraffe presented a rare opportunity not only to verify our neuromorphological findings in the adults (Jacobs et al., 2011, 2015), but also to document neuronal types early in development.

Although neocortical neuronal development has been extensively investigated in primates (Lund et al., 1977; Marin-Padilla, 1992; Travis et al., 2005; Bianchi et al., 2013; Elston and Fujita, 2014), rodents (Parnavelas et al., 1978; Miller, 1981) and, to a lesser extent, felines (Marin-Padilla, 1971, 1972), there is little neurodevelopmental information for other, relatively large brained species (Manger, 2008). Giraffes and especially elephants have prolonged developmental periods, with substantial increases in brain size from the neonate to the adult. In giraffes, biological measures indicate that sexual maturity is reached at ~4–5 years of age (Hall-Martin et al., 1978). In elephants, sexual maturity is reached at ~15 years of age, although successful reproduction for males can take 10–20 more years (Millar and Zammuto, 1983; Moss and Lee, 2011). Prolonged postnatal neurodevelopmental periods are also common in many mammals (Sacher and Staffeldt, 1974). Thus, given the relatively immature size of the newborn brains examined in the present study, we expected the neurons in our sample to be significantly smaller than their adult counterparts.

Based on our previous examination of neurons in adult giraffe and elephant neocortex (Jacobs et al., 2011, 2015), two other predictions follow. Quantitatively, as was the case with the adult animals, we expected the dendritic systems within the same neuronal type to be more extensive in the newborn elephant than in the newborn giraffe. Qualitatively, the newborn samples allowed us to investigate whether the fundamental neuromorphological differences we observed between the adult elephant and giraffe also obtained in newborn animals. In general, we expected the newborn giraffe neocortex to exhibit a more typical columnar organization, with vertically ascending apical dendrites, than the newborn elephant neocortex, which would be characterized by widely bifurcating apical dendrites and a greater variety of neuronal morphologies that are unlike those characteristic of anthropoid primate and murid rodent models. In contrast, little variation was expected for local circuit neurons (e.g., interneurons, neurogliaform, and Cajal–Retzius neurons) between the two species, as these neurons have been shown to be relatively uniform and morphologically conserved across eutherian mammals (Hof et al., 1999; Sherwood et al., 2009).

MATERIALS AND METHODS

Specimens

Cortical samples were obtained from a newborn giraffe (*Giraffa camelopardalis tippelskirchi*) and a newborn African elephant (*Loxodonta africana*). The brain of a 1-day old female giraffe with failure to thrive (378 g; autolysis time [AT] = 6 hours) was provided by the Cleveland Metroparks Zoo. The brain of a stillborn male elephant (1,745 g; AT < 12 hours) was provided by the Alabama Veterinary Diagnostic Laboratories, Auburn. Both brains were immersion-fixed in 10% formalin (giraffe: 30 days; elephant: ~10 months). Cortical areas of interest were removed and stored in 0.1 M phosphate-buffered saline (PBS) with 0.1% sodium azide for 3 months prior to Golgi staining. The present study was approved by the Colorado College Institutional Review Board (#011311-1).

Tissue selection

In the giraffe, tissue blocks (3–5 mm thick) were removed from the primary motor and visual cortices of the right hemisphere (Fig. 1). Motor cortex tissue was located anteriorly on the dorsomedial aspect of the cerebrum (Badlangana et al., 2007), and was removed about 1–2 cm lateral to the longitudinal fissure; visual cortex tissue was located posteriorly on the dorsomedial aspect of the cerebrum and was removed about 2–3 cm lateral to the longitudinal fissure (Fig. 1). In the elephant, tissue blocks (3–5 mm thick) were removed from the frontal, motor, and occipital (i.e., putative

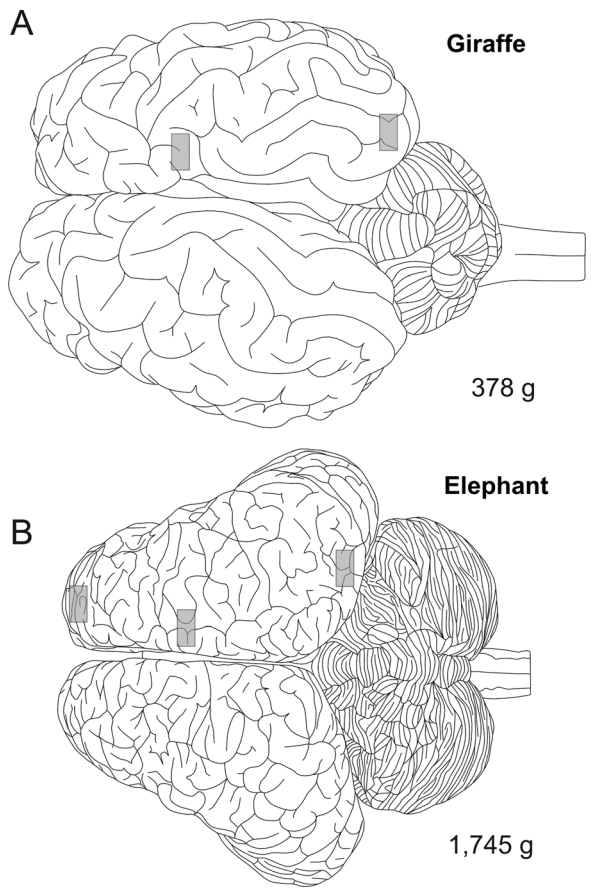

Figure 1. Dorsal views of the newborn giraffe (**A**) and newborn elephant (**B**) brains illustrating the relative position of tissue blocks removed for staining. Specifically, tissue was removed from the motor and visual cortices in the newborn giraffe, and frontal, motor, and occipital cortices in the newborn elephant. Images are based on adult brains as the newborn brains were too fragmented for accurate drawings. Therefore, only brain weights are provided.

visual) cortices of the right hemisphere (Jacobs et al., 2011). Frontal cortex tissue was located anterior to the orbital gyri (Jacobs et al., 2011) and was removed 3–5 cm from the midline; motor cortex tissue was located anteriorly on the dorsomedial aspect of the neocortex and was removed about 1–2 cm lateral to the longitudinal fissure; occipital cortex tissue was located in the parieto-occipital contour near the midline and was removed 3–5 cm anterior to the cerebellum (Fig. 1).

Neuron selection and quantification

Tissue was stained by using a modified rapid Golgi technique (Scheibel and Scheibel, 1978b), coded to prevent experimenter bias, and sectioned serially at 120 μm with a vibratome (Leica VT1000S, Leica Microsystems). Adjacent sections (40 μm thick) of selected tissue were stained with 0.5% cresyl violet for cytoarchitectural comparisons (Fig. 2). Laminar and cortical thickness measures were determined by averaging measures of 10 different sampling locations for each region of interest (Table 1). Neuronal selection was based on established criteria (Roitman et al., 2002; Jacobs et al., 2011, 2015; Lu et al., 2013), which required an isolated soma near the center of the 120-μm-thick section, with as fully impregnated, unobscured, and complete dendritic arbors as possible, with no beading or interruptions. To provide a comprehensive morphological analysis, neurons were selected to encompass representative typologies in each species.

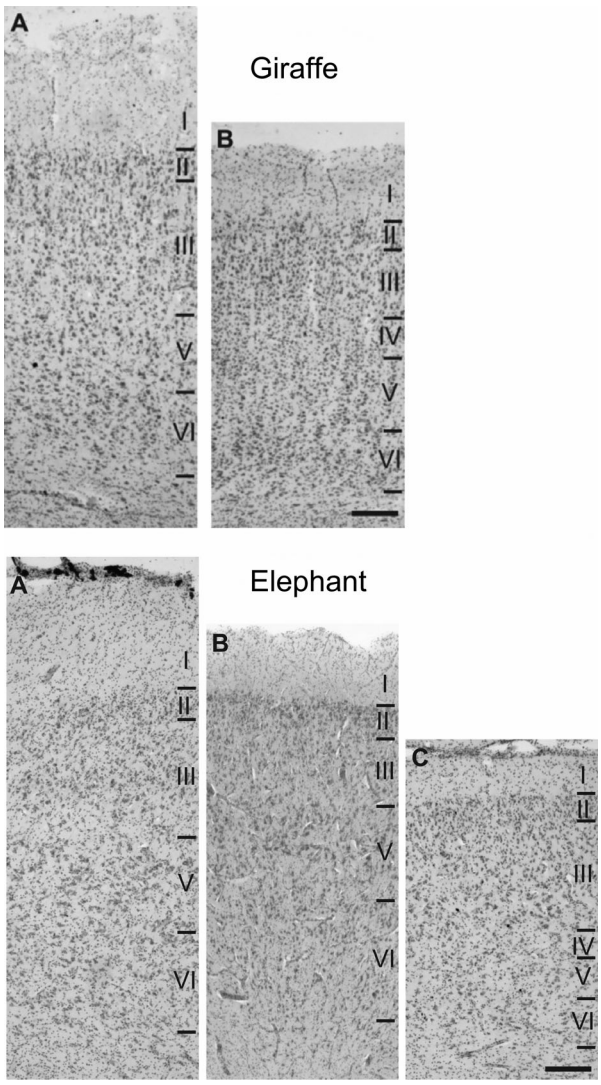

Figure 2. Photomicrographs of Nissl-stained cortical areas from the newborn giraffe and newborn elephant. In the giraffe, two regions were examined: motor (**A**) and visual (**B**) cortex. In the elephant, three regions were examined: frontal (**A**), motor (**B**), and occipital (**C**) cortex. Scale bar = 300 μm in Giraffe B (applies to A,B) and Elephant C (applies to A–C).

TABLE 1.
Laminar and Cortical Thickness (mean ± SD, μm)

Newborn giraffe	Motor cortex	Visual cortex
Layer I	803 ± 74	465 ± 34
Layer II	203 ± 11	203 ± 8
Layer III	832 ± 69	431 ± 21
Layer IV	–	261 ± 14
Layer V	484 ± 18	469 ± 19
Layer VI	537 ± 17	393 ± 37
Gray/white matter junction	2,859 ± 152	2,221 ± 177

Newborn elephant	Frontal cortex	Motor cortex	Occipital cortex
Layer I	723 ± 51	337 ± 25	261 ± 21
Layer II	212 ± 7	144 ± 24	187 ± 13
Layer III	772 ± 62	407 ± 55	733 ± 96
Layer IV	–	–	202 ± 17
Layer V	634 ± 25	401 ± 129	261 ± 30
Layer VI	671 ± 41	625 ± 53	320 ± 22
Gray/white matter junction	3,012 ± 206	1,913 ± 86	1,964 ± 138

Neurons were quantified under a planachromatic 60× oil objective along x-, y-, and z-coordinates using a Neurolucida system (MBF Bioscience, Williston, VT; RRID:nif-0000–10294), interfaced with an Olympus BH-2 microscope equipped with a Ludl XY motorized stage (Ludl Electronics, Hawthorne, NY) and a Heidenhain z-axis encoder (Schaumburg, IL). A MicroFire Digital CCD 2-Megapixel camera (Optronics, Goleta, CA) mounted on a trinocular head (model 1-L0229, Olympus, Center Valley, PA) displayed images on a 1,920 × 1,200 resolution Dell E248WFP 24-inch LCD monitor. Somata were first traced at their widest point in the two-dimensional plane to provide an estimate of cross-sectional area. Then, dendrites were traced somatofugally in their entirety while accounting for dendritic diameter and quantity of spines. Dendritic arbors were not traced into neighboring sections; broken ends and indefinite terminations were labeled as incomplete endings. Neurons with sectioned segments were not differentially analyzed because elimination of such tracings would have biased the sample toward smaller neurons (Schadé and Caveness, 1968; Uylings et al., 1986). When present, axons were also traced, although they typically disappeared after a short distance.

Neurons were traced by one observer (LL). Intrarater reliability was assessed by having this observer trace the same soma and dendritic branch 10 times. The average coefficient of variation for soma size (3.5%), total dendritic length (TDL; 0.8%), and dendritic spine number (DSN; 4.3%) indicated that tracings varied little. Intrarater reliability was further tested with a split plot design ($\alpha = 0.05$), which revealed no significant difference between the first and last five tracings. For interrater reliability, tracings of 10 different dendritic systems were compared with the same tracings done by the primary investigator (BJ). This reliability test was performed to ensure consistency with previous studies. Interclass correlations across soma size, TDL, and DSN (described below) averaged 0.99, 1.00, and 0.98, respectively. An analysis of variance (ANOVA; $\alpha = 0.05$) indicated that there was no significant difference between the two observers for the three measures. Furthermore, the primary investigator re-examined all completed tracings under the microscope to ensure accuracy.

Neuron descriptions and dependent dendritic and spine measures

Descriptively, neurons were classified according to somatodendritic criteria (Ferrer et al., 1986a,b; Jacobs et al., 2011, 2015) by considering factors such as soma size and shape, presence of spines, laminar location, and general morphology. Quantitatively, a centrifugal nomenclature was used to characterize branches extending from the soma as first-order segments, which bifurcate into second- and then third-order segments, and so on (Bok, 1959; Uylings et al., 1986). In addition to quantifying soma size (i.e., surface area, μm^2) and depth from the pial surface (μm), we examined six other measures that have been analyzed in previous studies (Jacobs et al. 2011, 2015): dendritic volume (Vol; μm^3; the total volume of all dendrites); total dendritic length (TDL; μm; the summed length of all dendritic segments); mean segment length (MSL; μm; the average length of each dendritic segment); dendritic segment count (DSC; the number of dendritic segments); dendritic spine number (DSN; the total number of spines on dendritic segments); and dendritic spine density (DSD; the average number of spines per μm of dendritic length). Dendritic branching patterns were also analyzed by using a Sholl analysis (Sholl, 1953), which quantified dendritic intersections at 20-μm intervals radiating somatofugally. All descriptive measures are presented as mean ± standard deviation (SD) unless noted otherwise.

Statistical analysis of species differences

The small number of neurons traced in each cortical area for each species precluded statistical analysis of regional differences, as has been done in primates (Travis et al., 2005; Bianchi et al., 2013). As a result, we provide here only a Golgi-dependent snapshot of the general distribution of neurons. Quantified neurons (N = 153) included 84 from the giraffe (motor: 46, visual: 38) and 69 from the elephant (frontal: 17, motor: 21,

occipital: 31). For reasons detailed extensively elsewhere (Jacobs et al., 2014), there are several limitations involved in parametric examination of such small neuromorphological datasets that are not normally distributed.

To determine whether elephant and giraffe infants could be differentiated from each other, we grouped the newborn neurons into two general categories: projection neurons (including pyramidal, magnopyramidal, gigantopyramidal, extraverted, flattened pyramidal, large fusiform, nonpyramidal multipolar, inverted pyramidal, horizontal pyramidal, and crab-like neurons; $n = 107$) and local circuit neurons (including interneurons, neurogliaform, and Cajal–Retzius neurons; $n = 46$). We then examined species differences in dependent measures for these two neuron groups using MARSplines, or Multivariate Adaptive Regression Splines (Statistica, release 12; StatSoft, Austin, TX; Friedman, 1991; Hastie et al., 2009), a nonparametric approach that is robust to violations of normality and extreme differences in variability.

RESULTS

Overview

Nissl-stained sections indicated that the frontal cortex in the elephant was the thickest of all regions (as measured from pia to white matter), and that motor cortices in both species were considerably thicker than putatively visual regions (Fig. 2). Although layer IV was present in the visual cortex of the giraffe, it was incipient in elephant occipital cortex, and absent in elephant motor and frontal cortices. The relative thickness of all layers across cortical regions for both species is provided in Table 1, which indicates that layers I, III, and VI were generally thicker than the other layers. The overall high quality of Golgi preparations is evident in photomicrographs (Figs. 3–7), which reveal well-impregnated, relatively complete dendritic systems. In the newborn giraffe neocortex, the most prominent neuron type was the pyramidal neuron. In contrast, atypical nonpyramidal multipolar neurons, which often possessed multiple, widely diverging apical dendrites, were the most common neuron type observed in the newborn elephant neocortex. In both species, local circuit neurons were mainly observed in deep cortical layers and, unlike their aspiny adult counterparts, were generally spiny, although less so than were projection neurons in both species. Individual tracings of neurons are presented for each cortical region in Figures 8 and 9 for the newborn giraffe, and Figures 10–12 for the newborn elephant. When more than five neurons of a particular type were traced, their relative location within the gyrus (e.g., gyral crown, sulcal wall, depth of sulcus) was noted, although such Golgi-based distributions should be interpreted cautiously. Quantitative data for all neuron types in both species are presented in Table 2 along with the number of each neuron type traced. Overall, newborn elephant neurons had more extensive dendrites (particularly in terms of Vol) than those in the newborn giraffe. Sholl analyses for each neuron type are presented in Figure 13. Below, we provide more detailed descriptions of each neuron type based on examination of all Golgi-stained sections as well as the particular neurons that were quantified.

Projection neurons

Pyramidal neurons

These were the most prominent neuron type traced in the newborn giraffe (soma depth range: 505–2,763 μm), but not in the newborn elephant (soma depth range: 883–2,450 μm; Table 2; Figs. 3C,H, 4B,D,I, 5A, 8A–H, 9A–G, 10A–C, 11A, 12B–D). In both species, traced pyramidal neurons were located relatively evenly across the gyral crown and sulcal wall. Pyramidal neuron somata were 141% larger in the elephant ($M_{\text{soma size}} = 680\ \mu m^2$) than in the giraffe ($M_{\text{soma size}} = 282\ \mu m^2$). In both species, somata were typically triangular in shape with basilar dendrites (giraffe: 4.6/neuron; elephant 6.1/neuron) radiating in all directions and a single apical dendrite extending vertically toward the pial surface. In the giraffe, more superficial pyramidal neurons frequently exhibited diverging apical dendrites, whereas deeper neurons exhibited long apical dendrites with fewer bifurcations. In the elephant, most apical dendrites bifurcated shortly after ascending from the apex of the soma. Dendrites were relatively spiny in both species (giraffe: DSD = 0.71; elephant: DSD = 0.64; Table 2). Sholl analysis suggested a similar dendritic profile for pyramidal neurons in both species (Fig. 13E,F,O). Nevertheless, dendritic measures for pyramidal neurons in the elephant tended to be considerably higher (by 276% for Vol.; 64% for TDL; 35% for MSL; 16% for DSC; 39% for DSN) than those observed in the giraffe, except for DSD, which was 11% higher in the giraffe.

Magnopyramidal neurons

These neurons, located only in the visual cortex, were the deepest neuron type in the newborn giraffe (soma depth range: 958–1,837 μm) and elephant (soma depth: 1,865 μm; Table 2; Figs. 4C, 9R–T, 12F). Although similar in morphology to pyramidal neurons, soma size and dendritic extent were greater in magnopyramidal neurons. In the giraffe, magnopyramidal neurons were 99% greater in soma size and 71% greater in TDL than pyramidal neurons (Table 2). In the elephant, magnopyramidal neurons were 18% greater in soma size and 41% greater in TDL than pyramidal neurons. Magnopyramidal neurons had an

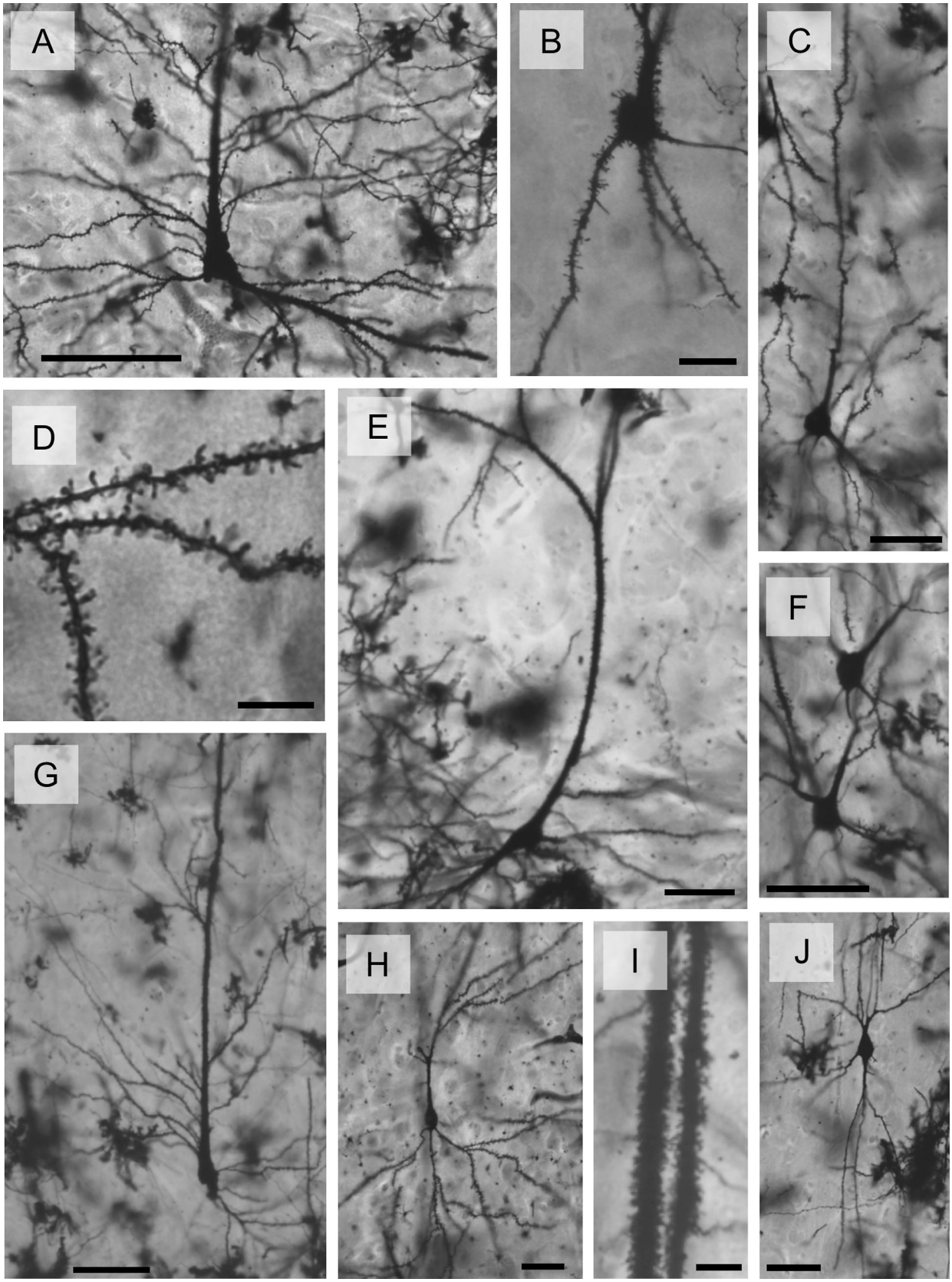

Figure 3. Photomicrographs of Golgi-stained neurons in the newborn giraffe motor cortex: gigantopyramidal neurons (**A,E,G**, see also Fig. 8R); interneurons (**B,J**); pyramidal neurons (**C,H**, see also Fig. 8H); higher magnification of basilar (**D**) and apical (**I**) dendritic segments; extraverted neuron (**F**, see also Fig. 8O,P). Scale bar = 100 μm in A,G; 20 μm in B; 50 μm in C,E,F,H,J; 10 μm in D,I.

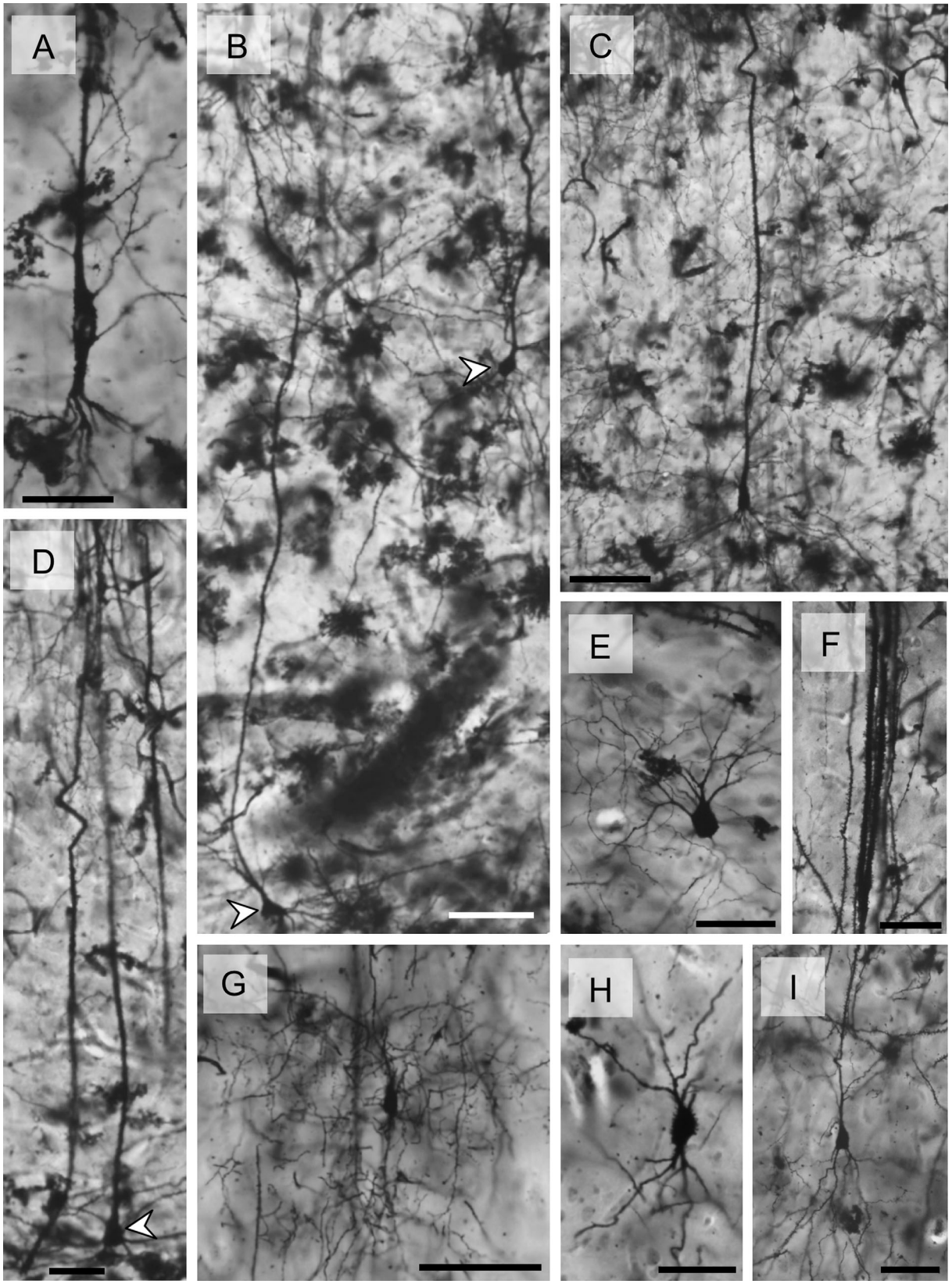

Figure 4. Photomicrographs of Golgi-stained neurons in the newborn giraffe visual cortex; large fusiform neuron (**A**, see also Fig. 9I); pyramidal neurons (**B**, see also Fig. 9B; **D,I**, see also Fig. 9D); magnopyramidal neuron (**C**, see also Fig. 9R); interneurons (**E,H**); higher magnification of apical dendritic segment (**F**); neurogliaform neuron (**G**, see also Fig. 9P). Arrowheads indicate somata of selected neurons. Scale bar = 50 μm in A,D–F,H,I; 100 μm in B,C,G.

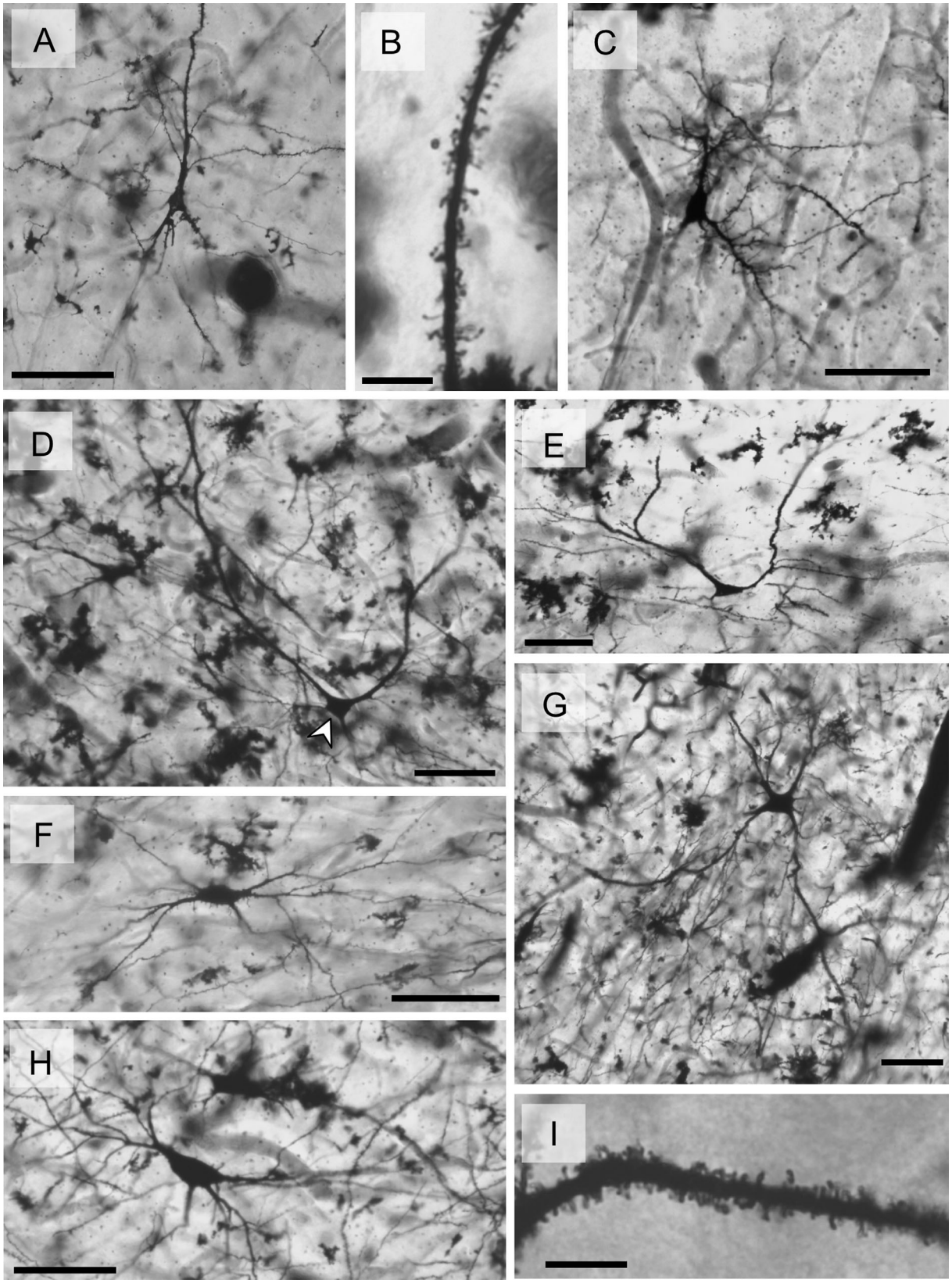

Figure 5. Photomicrographs of Golgi-stained neurons in the newborn elephant motor cortex: pyramidal neuron (**A**, see also Fig. 10B); higher magnification of basilar (**B**) and apical (**I**) dendritic segments; Cajal–Retzius neuron (**C**, see also Fig. 10G); nonpyramidal multipolar neurons (**D**, see also Fig. 10J; **G**, see also Fig. 10L); flattened pyramidal neuron (**E**, see also Fig. 10D); interneurons (**F**, see also Fig. 10N; **H**, see also Fig. 10O). Arrowheads indicate somata of selected neurons. Scale bar = 100 μm in A,C–H; 10 μm in B,I.

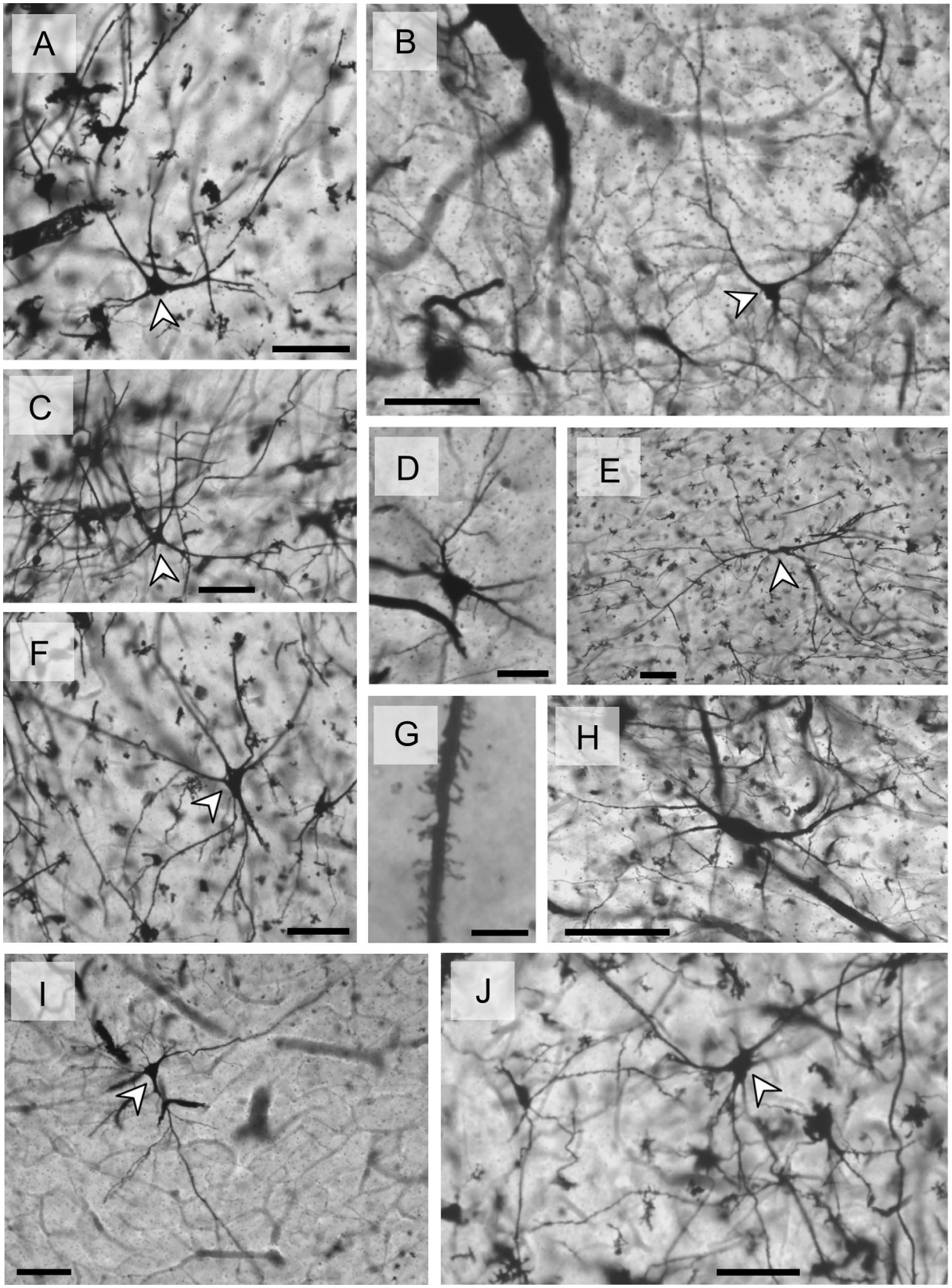

Figure 6. Photomicrographs of Golgi-stained neurons in the newborn elephant frontal cortex: nonpyramidal multipolar neurons (**A**, see also Fig. 11L; **B**, see also Fig. 11O; **C,J**, see also Fig. 11K); interneuron (**D**, see also Fig. 11I); flattened pyramidal neuron (**E**, see also Fig. 11F); inverted pyramidal neurons (**F**, see also Fig. 11G; **I**, see also Fig. 11H); higher magnification of basilar dendritic segment (**G**); crab-like neuron (**H**, see also Fig. 11B). Arrowheads indicate somata of selected neurons. Scale bar = 100 μm in A–C,E,F,H–J; 50 μm in D; 10 μm in G.

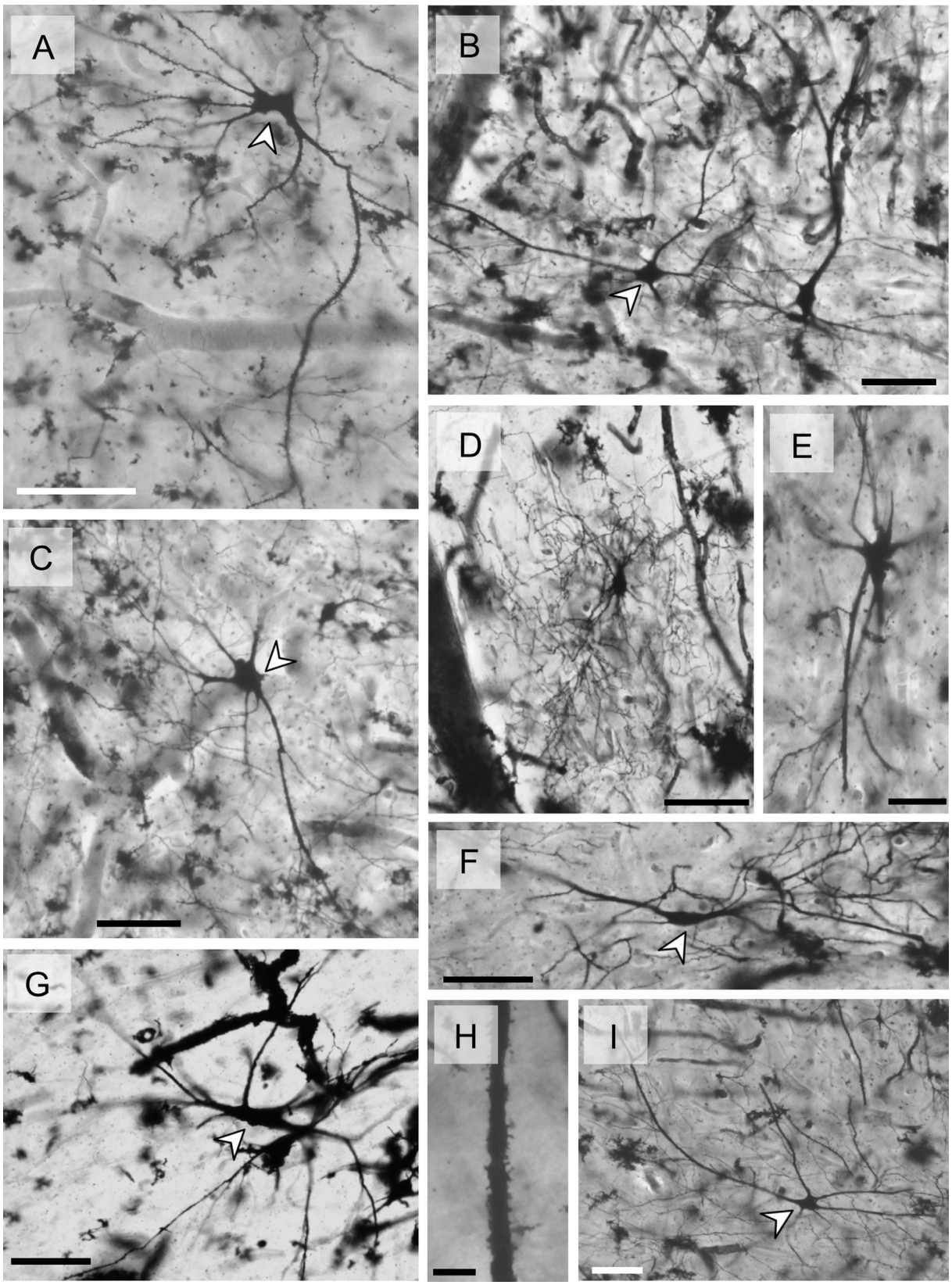

Figure 7. Photomicrographs of Golgi-stained neurons in the newborn elephant occipital cortex: nonpyramidal multipolar neurons (**A**, see also Fig. 12T; **B**, see also Fig. 12S; **C,I**, see also Fig. 12Q); neurogliaform neuron (**D**, see also Fig. 12G); inverted pyramidal neuron (**E**, see also Fig. 12A); flattened pyramidal neuron (**F**, see also Fig. 12P); interneuron (**G**, see also Fig. 12K); higher magnification of basilar dendritic segment (**H**). Arrowheads indicate somata of selected neurons. Scale bar = 100 μm in A–D,F,G,I; 50 μm in E; 10 μm in H.

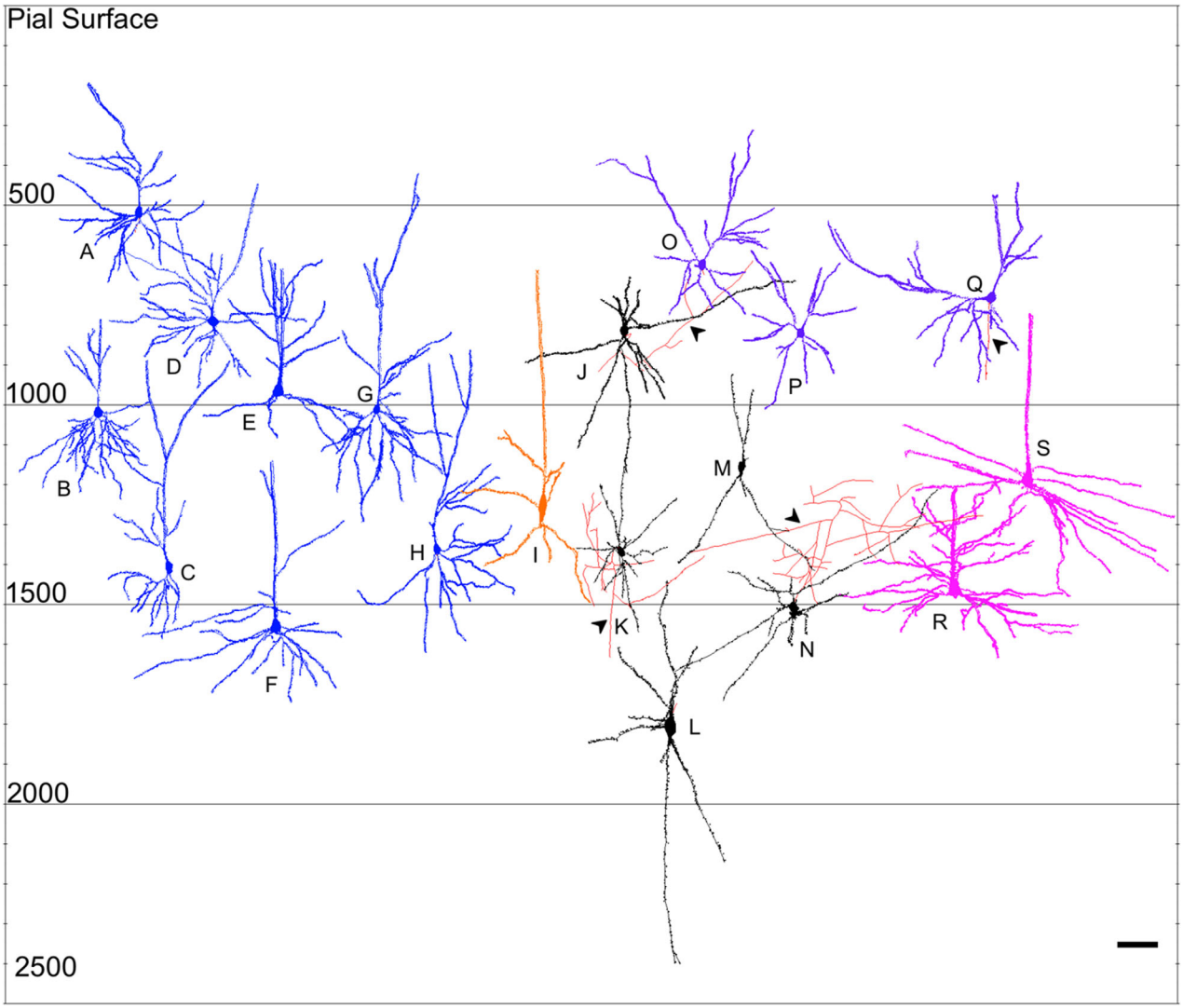

Figure 8. Neurolucida tracings of neurons in the newborn giraffe motor cortex indicating relative soma depth from the pial surface (in μm): pyramidal neurons (**A–H**); large fusiform neuron (**I**); interneurons (**J–N**); extraverted neurons (**O–Q**); gigantopyramidal neurons (**R,S**). Arrowheads indicate axons from neurons K, J, N, and Q. Scale bar = 100 μm. [Color figure can be viewed in the online issue, which is available at wileyonlinelibrary.com.]

average of 8.5 primary basilar dendrites/neuron in the giraffe and 4 primary basilar dendrites/neuron in the one neuron traced in the elephant. In terms of dendritic spines, magnopyramidal neuron DSD measures (giraffe: 0.60; elephant: 0.74) were similar to those observed in pyramidal neurons for both species (Table 2). Sholl analysis indicated greater dendritic complexity, especially in basilar dendrites, in magnopyramidal than in pyramidal neurons in both species (Fig. 13E,M). Although elephant dendritic measures for magnopyramidal neurons tended to be considerably higher (by 215% for Vol.; 35% for TDL; 30% for MSL; 5% for DSC; 65% for DSN; 23% for DSD) than those observed in the giraffe, it should be stressed that only one magnopyramidal neuron was traced in the elephant.

Gigantopyramidal neurons

These neurons were only documented in the motor cortex of the newborn giraffe and were located primarily along the sulcal wall (soma depth range 930–1,539 μm; Figs. 3A,E,G, 8R,S). These were also the largest neurons examined, with a Vol 45% greater than the magnopyramidal neurons (Table 2). Gigantopyramidal somata ($M_{\text{soma size}} = 710\ \mu m^2$) were morphologically similar to, but 152% larger than, those of pyramidal neurons. They possessed a single, long apical dendrite that extended vertically toward the pial surface. Basilar dendrites (8.4/neuron) extended in parallel approximately 200–300 μm from the soma, perpendicular to the apical dendrites, resembling the perisomatic, circumferential dendrites noted in human Betz cells (Scheibel and Scheibel,

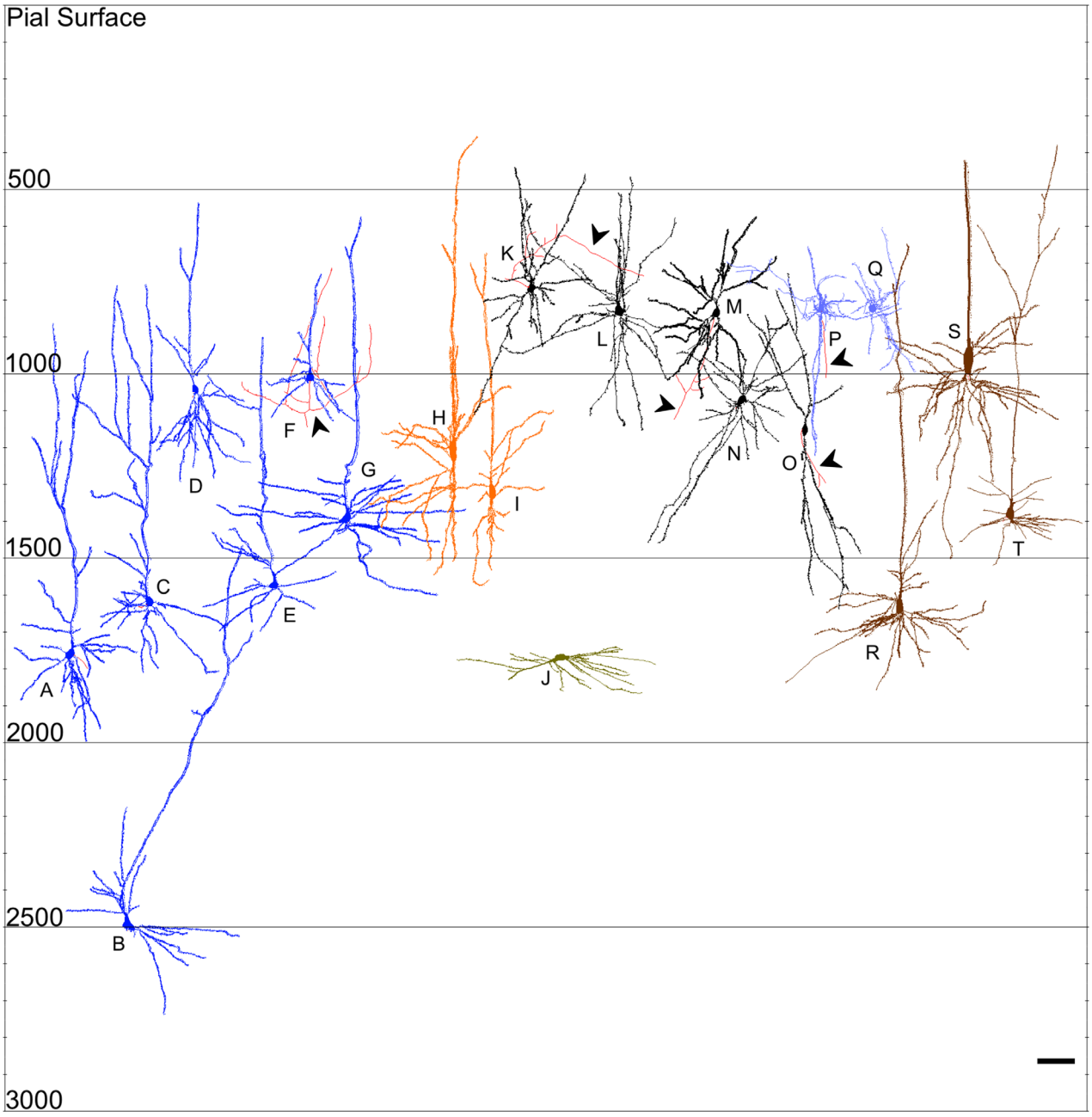

Figure 9. Neurolucida tracings of neurons in the newborn giraffe visual cortex indicating relative soma depth from the pial surface (in μm): pyramidal neurons (**A–G**); large fusiform neurons (**H,I**); horizontal pyramidal neuron (**J**); interneurons (**K–O**); neurogliaform neurons (**P,Q**); magnopyramidal neurons (**R–T**). Arrowheads indicate axons from neurons F, K, M, O, and P. Scale bar = 100 μm. [Color figure can be viewed in the online issue, which is available at wileyonlinelibrary.com.]

1978a). In the newborn giraffe, gigantopyramidal neurons were the most densely spined neurons analyzed (DSD = 0.83; Table 2) and Sholl analysis illustrated the highest dendritic peak of all neurons (Fig. 13B).

Extraverted neurons

An extraverted morphology was also only observed in the newborn giraffe motor cortex (Figs. 3F, 8O–Q), mostly in the crown of the gyrus. These were one of the most superficial neurons (soma depth range: 666–1,054 μm), with an average soma size of 251 μm^2 (Table 2). Somata were typically globular in shape, with an average of 2.7 primary basilar dendritic processes per neuron. Apical dendrites bifurcated near or on the soma into two individual branches that extended toward the pial surface. Dendrites were short, as indicated by their relatively low TDL (2,502 μm) and by the Sholl analysis (Fig. 13A), but spiny (DSD = 0.77; Table 2).

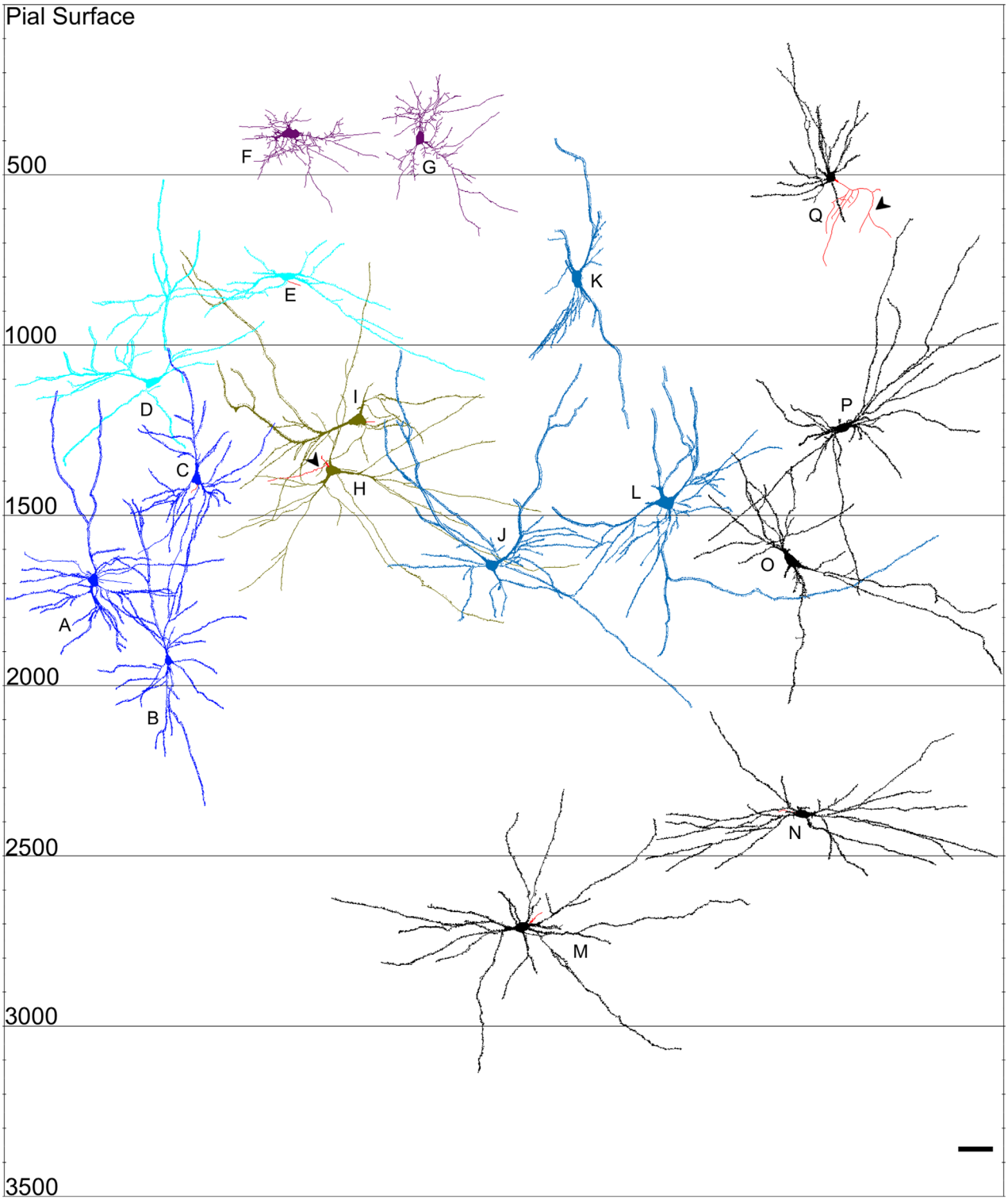

Figure 10. Neurolucida tracings of neurons in the newborn elephant motor cortex indicating relative soma depth from the pial surface (in μm): pyramidal neurons (**A–C**); flattened pyramidal neurons (**D,E**); Cajal–Retzius neurons (**F,G**); inverted pyramidal neurons (**H,I**); nonpyramidal multipolar neurons (**J–L**); interneurons (**M–Q**). Arrowheads indicate axons from neurons H and Q. Scale bar = 100 μm. [Color figure can be viewed in the online issue, which is available at wileyonlinelibrary.com.]

Flattened pyramidal neurons

These neurons were only found in the newborn elephant cortex, mostly along the sulcal wall (soma depth range: 795–1,956 μm; Table 2; Figs. 5E, 6E, 7F, 10D,E, 11C–F, 12N–P). Somata were shaped like relatively flattened triangles ($M_{soma\ size}$ = 774 μm^2; Table 2), with an

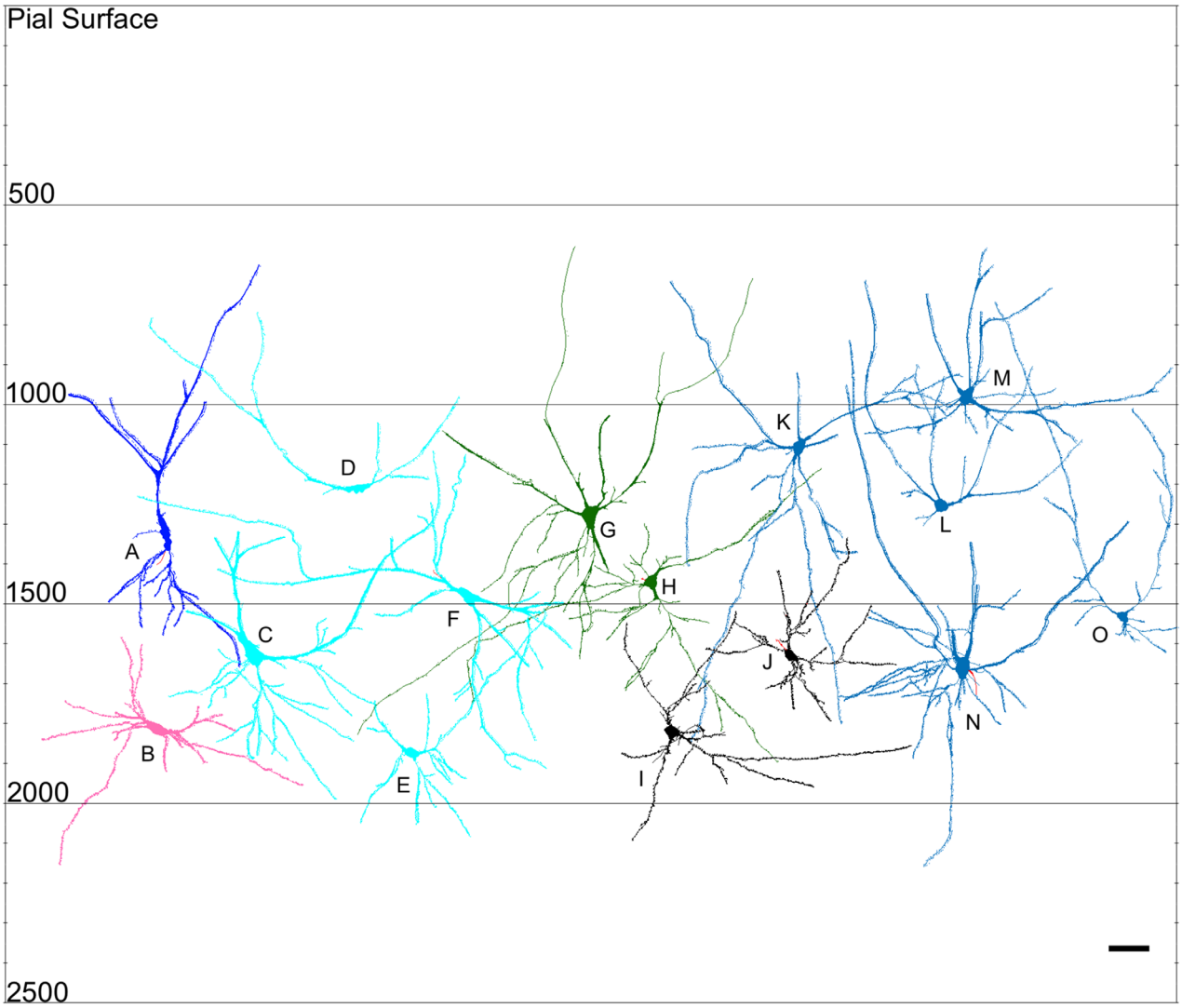

Figure 11. Neurolucida tracings of neurons in the newborn elephant frontal cortex indicating relative soma depth from the pial surface (in μm): pyramidal neuron (**A**); crab-like neuron (**B**); flattened pyramidal neurons (**C–F**); inverted pyramidal neurons (**G,H**); interneurons (**I,J**); nonpyramidal multipolar neurons (**K–O**). Scale bar = 100 μm. [Color figure can be viewed in the online issue, which is available at wiley onlinelibrary.com.]

average of 2.9 primary basilar dendrites/neuron. Apical dendrites (1.9/neuron) extended widely from the soma and curved toward the pial surface. Dendrites were moderately spiny (DSD = 0.58; Table 2). In contrast to other neuron types, Sholl analysis indicated that apical dendrites in flattened pyramidal neurons were more complex than basilar dendrites (Fig. 13J).

Large fusiform neurons

These relatively large fusiform neurons were only observed in the newborn giraffe motor and visual cortices (Figs. 4A, 8I, 9H,I). Their somata were larger ($M_{\text{soma size}} = 485\ \mu m^2$) than those of pyramidal neurons, and were located deep in the cortex (soma depth range: 1,204–1,475 μm; Table 2). Large fusiform neurons displayed an average of 4.5 short, primary basilar dendrites/neurons, which tended to descend in parallel toward the underlying white matter. A single bifurcating apical dendrite traveled vertically toward the pial surface. The basilar dendrites of these neurons had more spines than the dendritic processes of most other neurons in the newborn giraffe cortex (DSD = 0.76; Table 2). Sholl analysis indicated a similar dendritic length to that of pyramidal neurons in the newborn giraffe (Fig. 13D).

Nonpyramidal multipolar neurons

These were the most commonly observed projection neurons in the newborn elephant neocortex, and were located primarily along the sulcal wall (Figs. 5D,G,

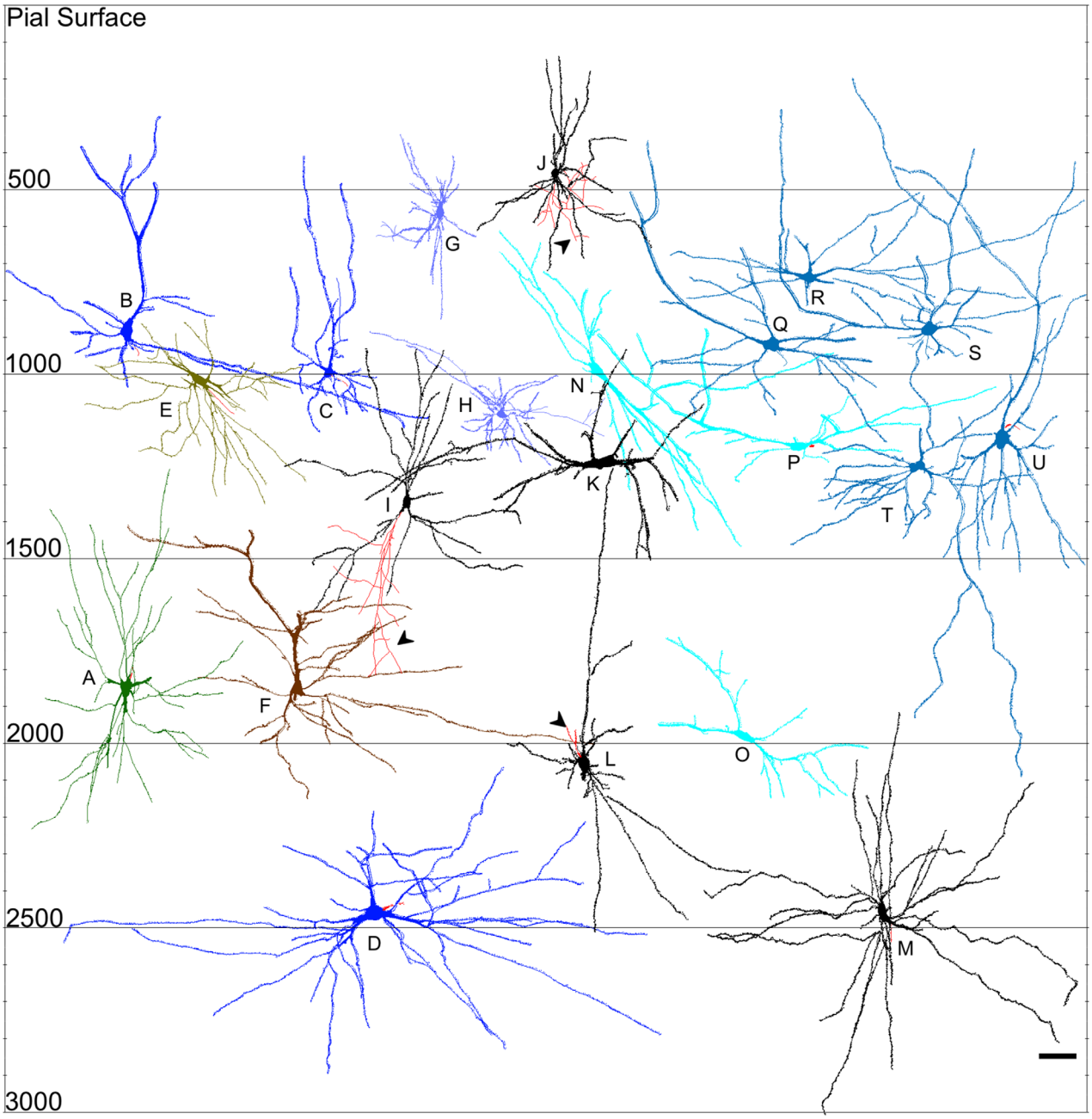

Figure 12. Neurolucida tracings of neurons in the newborn elephant occipital cortex indicating relative soma depth from the pial surface (in μm): inverted pyramidal neuron (**A**); pyramidal neurons (**B–D**); horizontal pyramidal neuron (**E**); magnopyramidal neuron (**F**); neurogliaform neurons (**G,H**); interneurons (**I–M**); flattened pyramidal neurons (**N–P**); nonpyramidal multipolar neurons (**Q–U**). Arrowheads indicate axons from neurons I, J, and L. Scale bar = 100 μm. [Color figure can be viewed in the online issue, which is available at wileyonlinelibrary.com.]

6A–C, 6J, 7A–C,I, 10J–L, 11K–O, 12Q–U). Because there was no clear directional orientation for these neurons, and because apical and basilar dendrites were difficult to differentiate, these neurons were, at the most general level, categorized as nonpyramidal multipolar neurons. Located between 712 and 1,741 μm from the pial surface, somata were typically globular in shape and relatively large ($M_{\text{soma size}} = 766\ \mu m^2$). On average, this neuron type exhibited 7.2 thick, primary dendritic processes (5.5 presumed to be basilar; 1.7 presumed to be apical) that branched outward from the soma. Based on dendritic arborization patterns, two subtypes of this multipolar neuron could be identified: multiapical and starfish. Multiapical neurons were characterized by the presence of what appeared to be several apical dendrites that generally ascended toward the pial

TABLE 2.

Summary Statistics (mean ±SEM) for Newborn Giraffe and Newborn Elephant Neurons

Type	No.[1]	Volume (μm ^{3})	Total dendritic length (μm)	Mean segment length (μm)	Dendritic segment count	Dendritic spine number	Dendritic spine density	Soma size (μm ^{2})	Soma Depth (μm) (range)
Projection neurons									
Giraffe									
Extraverted	9	4,697 ± 633	2,502 ± 351	70 ± 8	36 ± 4	1,921 ± 328	0.77 ± 0.06	251 ± 17	768 ± 41 (666–1,054)
Gigantopyramidal	7	24,152 ± 5,720	4,957 ± 375	89 ± 5	56 ± 5	4,095 ± 358	0.83 ± 0.04	710 ± 99	1,197 ± 83 (930–1,539)
Horizontal	1	6,575	3,201	82	39	1,384	0.43	258	1,740
Large fusiform	4	7,555 ± 2,073	3,127 ± 655	74 ± 14	47 ± 11	2,278 ± 527	0.76 ± 0.13	485 ± 66	1,305 ± 60
Magnopyramidal	4	16,613 ± 3,729	5,243 ± 747	81 ± 6	64 ± 4	3,181 ± 684	0.60 ± 0.09	561 ± 187	1,448 ± 188 (958–1,837)
Pyramidal	37	5,980 ± 528	3,066 ± 176	71 ± 3	44 ± 2	2,211 ± 170	0.71 ± 0.03	282 ± 14	1,235 ± 80 (505–2,763) (1,204–1,475)
Elephant									
Crab-like	1	10,743	2,595	70	37	1,251	0.48	869	1,815
Flattened	10	24,085 ± 5,077	4,177 ± 537	90 ± 7	47 ± 4	2,413 ± 348	0.58 ± 0.04	774 ± 136	1,341 ± 123 (795–1,956)
Horizontal	4	19,355 ± 1,070	5,029 ± 662	102 ± 12	51 ± 9	2,482 ± 278	0.51 ± 0.07	707 ± 63	1,122 ± 113 (886–1,360)
Inverted	3	21,544 ± 6,224	5,529 ± 777	89 ± 15	63 ± 4	2,898 ± 261	0.53 ± 0.03	808 ± 192	1,528 ± 170 (1,286–1,857)
Magnopyramidal	1	52,309	7,060	105	67	5,252	0.74	801	1,865
Non-pyramidal multipolar	17	24,953 ± 1,792	4,482 ± 350	96 ± 6	47 ± 4	2,518 ± 353	0.53 ± 0.04	766 ± 50	1,206 ± 83 (712–1,741)
Pyramidal	9	22,480 ± 4,919	5,021 ± 810	96 ± 7	51 ± 4	3,084 ± 369	0.64 ± 0.03	680 ± 112	1,438 ± 167 (883–2,450)
Local circuit neurons									
Giraffe									
Interneuron	20	3,837 ± 435	2,660 ± 234	79 ± 6	36 ± 3	900 ± 119	0.34 ± 0.03	276 ± 29	1,031 ± 68 (606–1,812)
Neuroglial	2	2,592 ± 339	2,744 ± 796	43 ± 2	64 ± 16	713 ± 272	0.25 ± 0.03	183 ± 9	808 ± 9 (799–816)
Elephant									
Cajal-Retzius	2	7,171 ± 574	51,000 ± 100	19 ± 4	281 ± 51	693 ± 230	0.14 ± 0.04	642 ± 136	398 ± 5 (393–404)
Interneuron	20	11,616 ± 1,839	4,670 ± 365	92 ± 8	53 ± 3	1,603 ± 170	0.34 ± 0.01	604 ± 64	1,607 ± 171 (477–3,079)
Neuroglial	2	6,283 ± 2,752	4,255 ± 289	59 ± 11	74 ± 9	1,019 ± 76	0.24 ± 0.03	271 ± 80	860 ± 243 (617–1,102)

[1]Number of neurons traced.

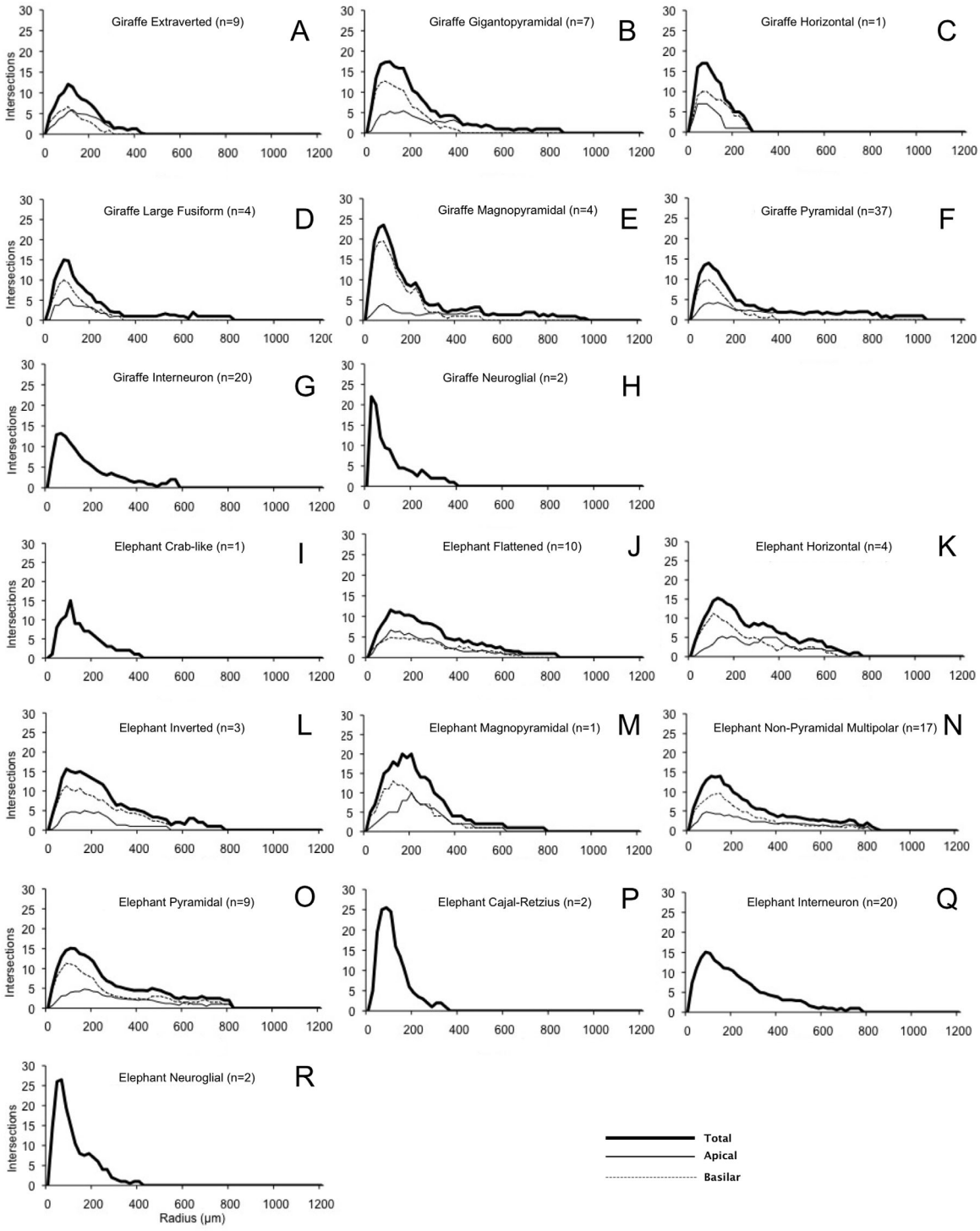

Figure 13. Sholl analyses of 8 neuron types in the newborn giraffe and 10 neuron types in the newborn elephant indicating relative apical, basilar, and total dendritic complexity of branching patterns. Dendritic intersections were quantified at 20-μm intervals using concentric rings. In the newborn giraffe, neurons **A–F** are projection neurons and **G, H** are local circuit neurons. In the newborn elephant, neurons **I–O** are projection neurons and **P–R** are local circuit neurons. Neuron types B, D–F, and all newborn elephant projection neuron types had relatively long apical dendrites whereas neuron types A and C had shorter apical dendrites. Apical dendrites either extended much further than the basilar dendrites (A,B,D–F) or were of similar length (C,I–O). For most neuron types, relative dendritic intersections peaked before 200 μm for both the basilar and apical dendrites; however, some neuron types in the newborn elephant had relative dendritic intersections peak closer to 200 μm than did neuron types in the newborn giraffe.

TABLE 3.

Descriptive Statistics by Neuron Classification and Species

Neuron type	Species	Measure	Count	Mean	Variance	Skew[1]	Kurtosis[1]
Projection neurons	Elephant	Vol	45	23,832.93	143,140,911	0.86	0.64
		TDL	45	4,655.81	3,003,993	1.05	2.93
		DSC	45	49.36	212	−0.08	−0.24
		MSL	45	95.43	550	1.02	2.44
		Soma size	45	751.24	82224	1.51	**4.82**
		DSN	45	2,662.58	1,535,222	0.66	0.11
		DSD	45	0.56	0	−0.04	−1.00
	Giraffe	Vol	62	8,642.84	71,188,331	**3.47**	**16.59**
		TDL	62	3,344.00	1,806,121	0.39	0.18
		DSC	62	45.39	227	0.08	−0.55
		MSL	62	73.84	320	−0.14	−0.40
		Soma size	62	356.34	42,519	2.27	**5.55**
		DSN	62	2,434.92	1,436,993	0.52	−0.36
		DSD	62	0.72	0	−0.25	−0.44
Local circuit neurons	Elephant	Vol	24	10,801.50	60,059,481	2.60	**8.74**
		TDL	24	4,671.60	2,245,675	1.21	2.57
		DSC	24	73.71	4,470	**3.29**	**10.86**
		MSL	24	83.52	1,512	0.32	0.03
		Soma size	24	579.50	77,989	1.54	**3.74**
		DSN	24	1,478.21	56,6530	1.52	**3.32**
		DSD	24	0.31	0	−0.94	0.42
	Giraffe	Vol	22	3,723.69	3,564,644	1.53	2.98
		TDL	22	2,667.23	1,051,124	0.88	0.34
		DSC	22	38.09	236	0.72	0.97
		MSL	22	75.94	723	−0.01	−1.37
		Soma size	22	268.92	16,416	**3.43**	**13.96**
		DSN	22	882.96	26,7293	1.62	4.38
		DSD	22	0.33	0	1.13	1.21

[1]**Bold numbers** represent measures with a skew or kurtosis over 3, indicating non-normal distributions.
Abbreviations: Vol, dendritic volume; TDL, total dendritic length; DSC, dendritic segment count; MSL, mean segment length; DSN, dendritic spine number; DSD, dendritic spine density.

surface. We labeled one of these multiapical neuron types as "starfish" neurons because they resembled the five-legged common starfish (*Asterias rubens*) insofar as they consistently possessed five thick dendritic processes, none of which were distinctly apical or basilar in appearance; these extended radially from the soma in all directions (e.g., Figs. 11K,M, 12Q,S,T). Although these qualitative distinctions were apparent, these subtypes of nonpyramidal multipolar neurons were not differentially analyzed. These neurons were moderately spiny (DSD = 0.53; Table 2), and Sholl analysis indicated that dendritic extension from the soma was among the longest in the newborn elephant cortex (Fig. 13N).

TABLE 4.

Correct–Incorrect Confusion Matrices for Differentiation of Newborn Species for Projection and Local Circuit Neurons

			Predicted			Predictor importance[1]					
		94.4% Correct[2]	Elephant	Giraffe	Row total	Vol	TDL	MSL	DSC	DSN	DSD
Projection neurons	Observed	Elephant	**41**	2	43	1	0	0	1	0	4
		Giraffe	4	**60**	64	Soma Size					
		Column total	45	62	107	3					
		93.5% Correct[2]	Elephant	Giraffe	Row total	Vol	TDL	MSL	DSC		
Local circuit neurons	Observed	Elephant	**21**	0	21	5	0	0	1		
		Giraffe	3	**22**	25	Soma Size					
		Column total	24	22	46	3					

[1]Predictor importance indicates how many times each neuronal measure was used in the regression analysis. See text for more details.
[2]**Bold numbers** represent the correct predictions. The percentage correct is calculated by dividing the sum of the two bold numbers by the total number of neurons examined. So, for the projection neurons: (41 + 60)/107 = 0.944.
Abbreviations: Vol, dendritic volume; TDL, total dendritic length; DSC, dendritic segment count; MSL, mean segment length; DSN, dendritic spine number; DSD, dendritic spine density.

Inverted pyramidal neurons

These neurons were only observed in the newborn elephant cortex, with a soma size that was 19% larger than pyramidal neurons (Table 2; Figs. 6F,I, 7E, 10H,I, 11G,H, 12A). Soma depths for these neurons ranged from 1,286 to 1,857 μm below the pial surface. Although qualitatively and quantitatively similar to pyramidal neurons in terms of morphology, inverted pyramidal neurons differed in orientation insofar as the apical dendrite descended toward the underlying white matter and basilar dendrites (5/neuron) extended toward the pial surface. These neurons were moderately spiny (DSD = 0.53). Sholl analysis indicated that this neuron type had the shortest apical dendritic length of all neuron types (Fig. 13L).

Horizontal pyramidal neurons

Pyramidal neurons with a horizontal orientation were documented relatively deeply in the visual cortex of the newborn giraffe (soma depth: 1,740 μm) and in the motor and occipital cortices of the newborn elephant (soma depth range: 886–1,360 μm; Table 2; Figs. 9J, 12E). Somata were 174% larger in the elephant ($M_{\text{soma size}} = 707$ μm^2) than in the giraffe ($M_{\text{soma size}} = 258$ μm^2). In both species, these neurons possessed triangular somata from which an apical dendrite extended laterally or obliquely (<45°), with several primary basilar dendrites/neuron (two in the giraffe; five in the elephant) radiating from the opposite pole of the soma. Horizontal pyramidal neurons in the giraffe (DSD = 0.43) were less spiny than most other neuron types. In the elephant, these were moderately spiny (DSD = 0.51; Table 2). Sholl analysis revealed that basilar dendrites were approximately the same length as apical dendrites in the newborn giraffe (Fig. 13C), but that basilar were longer than apical dendrites in the newborn elephant (Fig. 13K). Although elephant dendritic measures for horizontal pyramidal neurons tended to be considerably higher (by 194% for Vol; 57% for TDL; 24% for MSL; 31% for DSC; 79% for DSN; 19% for DSD) than those observed in the giraffe, it should be stressed that only one horizontal pyramidal neuron was traced in the giraffe.

In addition, only one crab-like neuron (Figs. 6H, 11B; Jacobs et al., 2011) was found in the frontal cortex of the newborn elephant. Located at a depth of 1,815 μm, the soma was round in shape with a total of five primary basilar dendrites radiating symmetrically from opposite sides of the soma. Dendrites were moderately spiny (DSD = 0.48; Table 2) compared with other neurons. Sholl analysis indicated that dendritic length was among the shortest of all neurons observed in the newborn elephant (Fig. 13I).

Local circuit neurons

Interneurons

These neurons were the most common local circuit neurons traced in both the giraffe (soma depth range: 606–1,812 μm) and the elephant (soma depth range: 477–3,079 μm), and were located relatively evenly from the apex of the gyrus to the depth of the sulcus (Table 2; Figs. 3B,J, 4E,H, 5F,H, 6D, 7G, 8J–N, 9K–O, 10M–Q, 11I,J, 12I–M). Somata were rounded and had an average of 5.2 primary dendrites/neuron in the giraffe, and 8.4 primary dendrites/neuron in the elephant. Two subtypes of interneurons were noted: 1) multipolar neurons (Figs. 3B,J, 4E,H, 5F,H, 6D, 7G, 8J–L,N, 9K–N), which exhibited an average of 5.6 primary dendrites/neuron in the giraffe and 8.4 primary basilar dendrites/neuron in the elephant; and 2) bipolar neurons (Figs. 8M, 9O), which had two dendritic segments extending in opposite directions. Sholl analysis indicated that interneurons had the highest dendritic length of all local circuit neurons in both species (Fig. 13G,Q). Dendritic measures for elephant interneurons neurons tended to be higher (by 203% for Vol; 76% for TDL; 16% for MSL; 47% for DSC) than those observed in the giraffe.

Neurogliaform neurons

This neuron type was found in the visual cortex of both the giraffe (soma depth range: 799–816 μm) and the elephant (soma depth range: 617–1,102 μm; Table 2; Figs. 4G, 7D, 9P,Q, 12G,H). In both species, somata were typically globular, with many fine, slightly beaded, radially distributed dendrites (giraffe: 8.5/neuron; elephant: 9/neuron) that tended to bifurcate near the soma. Sholl analysis indicated one of the lowest dendritic lengths of local circuit neurons in both species (Fig. 13H,R). As with interneurons, dendritic measures for elephant neurogliaform neurons tended to be higher (by 142% for Vol; 55% for TDL; 37% for MSL; 16% for DSC) than those observed in the giraffe.

Cajal–Retzius neurons

Only two of these cells, originally described by Retzius (1893) and Ramón y Cajal (1891), were observed superficially in the motor cortex of the elephant (soma depth range: 393–404 μm; Table 2; Figs. 5C, 10F,G). Radiating in all directions from an irregularly shaped soma was an average of 7.5 primary dendrites/neuron. These dendrites branched extensively and irregularly, resulting in the highest DSC (281; Table 2) of all neuron types. Sholl analysis exhibited the highest dendritic

complexity, but the lowest dendritic length of neurons in the newborn elephant (Fig. 13P).

Statistical analysis of species differences

After grouping individual neuron types into two categories, projection neurons and local circuit neurons, we examined elephant/giraffe mean ratios for each dependent variable to gain a descriptive understanding of the differences between species. With the exception of DSD in projection neurons, all ratios were larger for the elephant than the giraffe, especially for Vol and soma size (Table 3). However, the neuronal measures not only had variances ranging from just over 0 to more than 60 million, many of them also exhibited skew or kurtosis values over 3, indicating non-normal distributions that prevented the correct use of conventional parametric statistical tests (Table 3). We therefore used individual MARSplines analyses (Berk and Breedman, 2003) to predict species by neuronal measures for each class of neuron. For projection neurons, seven variables were considered (Vol, TDL, MSL, DSC, DSN, DSD, and soma size); for local circuit neurons, the two spine measures (DSN, DSD) were omitted because of their transient nature during development. The results from both MARSplines analyses (Table 4) rejected the null hypothesis of no differences between species for both projection neurons [$\chi^2_{(1)} = 83.79$, $P \leq 0.0000$] and local circuit neurons [$\chi^2_{(1)} = 35.42$, $P \leq 0.0000$]. Species were predicted with 94.4% accuracy for projection neurons, and 93.5% accuracy for local circuit neurons (Table 4). This procedure also provided a qualitative assessment of the relative importance of each predictor (i.e., Vol, TDL, soma size, etc.) in identifying whether a neuron belonged or did not belong to a particular species. Importance was measured by counting the number of times each neuronal measure was used by the regression analyses. For projection neurons, measures associated with differentiating newborn elephants from newborn giraffes were, from least to most important, DSC, Vol, soma size, and DSD; for local circuit neurons, the measures were Vol, soma size, and DSC (Table 4).

DISCUSSION

Grossly, the brains were considerably smaller than their adult counterparts. The newborn giraffe brain, at 378 g, was 27% below the adult average of 518 g (Mitchell et al., 2008) and the newborn elephant brain, at 1,745 g, was 64% below the adult average of 4,783 g (Shoshani et al., 2006). Morphologically, the present results indicate that the newborn giraffe and newborn elephant have a fundamentally different cortical organization, confirming that neuromorphological variation observed in the adults of these species is generated during prenatal brain development (Jacobs et al., 2011, 2015). Much like in other cetartiodactyls (Butti et al., 2014, 2015), giraffe neocortex is characterized by a predominance of pyramidal neurons with singular and/or narrowly bifurcating apical dendrites that contribute to a vertically oriented cortical architecture similar to that of primates and rodents (Valverde, 1986; Mountcastle, 1997). In contrast, African elephant neocortex exhibits a variety of large projection neurons with widely bifurcating apical dendrites that form V-shaped bundles, which differ considerably from the canonical vertical apical dendritic architecture of typical primate and rodent pyramidal neurons (Fleischhauer et al., 1972; Jacobs et al., 2011). Quantitatively, both projection and local circuit neurons in the newborn elephant also tended to be larger than corresponding neurons in the newborn giraffe, especially in terms of soma size and volume. Below, following a brief discussion of methodological issues, we explore these findings in more detail, with a focus on those aspects of neuronal morphology that appear particularly relevant to the newborn cortex.

Methodological considerations

The most evident limitation of the current study is the small sample size, in terms of both available brain specimens and the number of neurons reconstructed for quantification. Although we only had access to one brain from each species, the availability of optimally preserved postmortem brain tissue in newborns presented a unique opportunity to study developmental aspects of neuroanatomy in these uncommon animals. Such limited availability of tissue definitely affected our capacity to analyze a large number of neurons in each cortical region, considering the yield of the Golgi technique and our criteria for inclusion. However, we believe that the present dataset offers an important and informative overview of neocortical neuronal types at an early development stage in these large brained mammals, which overall contributes to a better knowledge of the rarely accessible neuroanatomy of these species.

More generally, the limitations of the Golgi technique have been extensively presented elsewhere and will not be addressed again here (Williams et al., 1978; Braak and Braak, 1985; Horner and Arbuthnott, 1991; Jacobs and Scheibel, 1993, 2002; Jacobs et al., 1997, 2011, 2014, 2015). More specific to the present study are problems associated with determining the presence or absence of neuron types based on Golgi impregnations (Jacobs et al., 2014, 2015). At best, one can make only general, relative observations about the number or

distribution of particular neuronal types, especially given the limited number of neurons sampled in the present study. Furthermore, there are issues related to classification of neurons (Germroth et al., 1989; Masland, 2004; Bota and Swanson, 2007; DeFelipe et al., 2013) based solely on somatodendritic architecture (Nelson et al., 2006; Ascoli et al., 2008). This is particularly true for the (presumed) projection neurons in the elephant, whose morphology does not strictly conform to the Euarchontoglires-centric nomenclature in the literature (Manger et al., 2008; Jacobs et al., 2011). Therefore, classification of neuronal subtypes in the present study should be seen as tentative, with more definitive phenotypic verification requiring molecular techniques (Molnár and Cheung, 2006; Simat et al. 2007). Such immunohistochemical investigations are in progress for several species (e.g., elephant, minke whale) that we have already examined with the Golgi technique. Nevertheless, the present results may be compared with those obtained in the adults of the same species, allowing for an examination of developmental changes in neuromorphology.

Projection neurons

Newborn projection neuron morphology was nearly identical to that observed in the adults of both species (Jacobs et al., 2011, 2015). Several neuronal types (e.g., pyramidal, magnopyramidal, gigantopyramidal, large fusiform neurons), particularly in the giraffe, conformed to existing descriptions of typical projection neurons, with newborn dendritic morphology similar to that observed in several species: rats (Miller, 1981), cats (Noback and Purpura, 1961; Marin-Padilla, 1972), rabbits (Globus and Scheibel, 1967), and humans (Takashima et al., 1981; Marin-Padilla, 2014). In the present study, magnopyramidal neurons appeared to be scaled-up pyramidal neurons with a similar morphology but a larger number of basilar dendrites. In contrast, gigantopyramidal neurons were not only larger than magnopyramidal neurons, but also exhibited the distinctive perisomatic, circumferential dendrite characteristics of Betz cells (Betz, 1874; Scheibel et al., 1974; Scheibel and Scheibel, 1978a). In newborn elephant pyramidal-like neurons, however, the apical dendrites tended to bifurcate, a prominent characteristic observed in the adult African elephant cortex (Jacobs et al., 2011). Such apical dendritic architecture resembled that of extraverted neurons (Sanides and Sanides, 1972; Fitzpatrick and Henson, 1994; Sherwood et al., 2009), which were prominent in the superficial cortical layers in the newborn giraffe. These widely bifurcating apical branches in elephant pyramidal neurons and in extraverted neurons may be a consequence of thalamocortical input to superficial layers of agranular cortex (Ferrer and Perera, 1988; Glezer and Morgane, 1990), and may facilitate communication across wider cortical regions (Hof and Van der Gucht, 2007).

Although pyramidal neurons appear to be the most intensively investigated of all neuron types in the neocortex among newborn mammals of different species, methodological differences across studies complicate direct quantitative comparison. One investigation methodologically identical to the present, however, quantified the basilar dendrites of layer V pyramidal neurons in neonatal humans (Travis et al., 2005). In this sample of four human neonates, soma size (ranging from 318 μm^2 in Brodmann area 10 to 482 μm^2 in area 4) was less than the soma size in newborn elephant pyramidal neurons, but greater than that observed in the giraffe. In terms of basilar dendrites in neonatal humans, TDL ranged from 2,291 μm in area 10 to 4,733 μm in area 4; DSN ranged from 573 in area 10 to 1,720 in area 4. In the current study, basilar dendritic values in newborn elephant pyramidal neurons (TDL = 3,260 μm; DSN = 1,901) were similar to those values observed in neonatal humans. For basilar dendrites in the newborn giraffe (TDL = 1,715 μm; DSN = 1,189), TDL was lower, but DSN was within the range observed in human neonates. In other, methodologically different studies on human neonates, it appears that newborn giraffe and especially elephant pyramidal neurons tend to have more dendritic complexity, as measured by both TDL and DSC, than neonatal human pyramidal neurons in both occipital and prefrontal cortex (Becker et al., 1984; Petanjek et al., 2008). When compared with young control rats, TDL appears much greater in newborn elephants and giraffes (Bock et al., 2005). DSD values, however, appear similar to those in newborn elephants and giraffes in rats between 15 and 23 days of age (Miller, 1981; Murmu et al., 2006).

Two types of atypically oriented pyramidal neurons were documented in the present study: inverted and horizontal (Ramón y Cajal, 1891; Miller, 1988). As in the adult, horizontal but not inverted pyramidal neurons stained in the newborn giraffe (Jacobs et al., 2015), whereas both neuron types were observed in the elephant (Jacobs et al., 2011). Similar to typical pyramidal neurons, morphogenesis of atypically oriented pyramidal neurons progresses in an inside-to-outside sequence, with deeper neurons maturing before more superficial neurons (Miller, 1988). Although these atypically oriented pyramidal neurons were once considered to be aberrant (Van der Loos, 1965; Landrieu and Goffinet, 1981), they have now been documented in a variety of species (e.g., rats, rabbits, cats, sheep, sloths, anteaters,

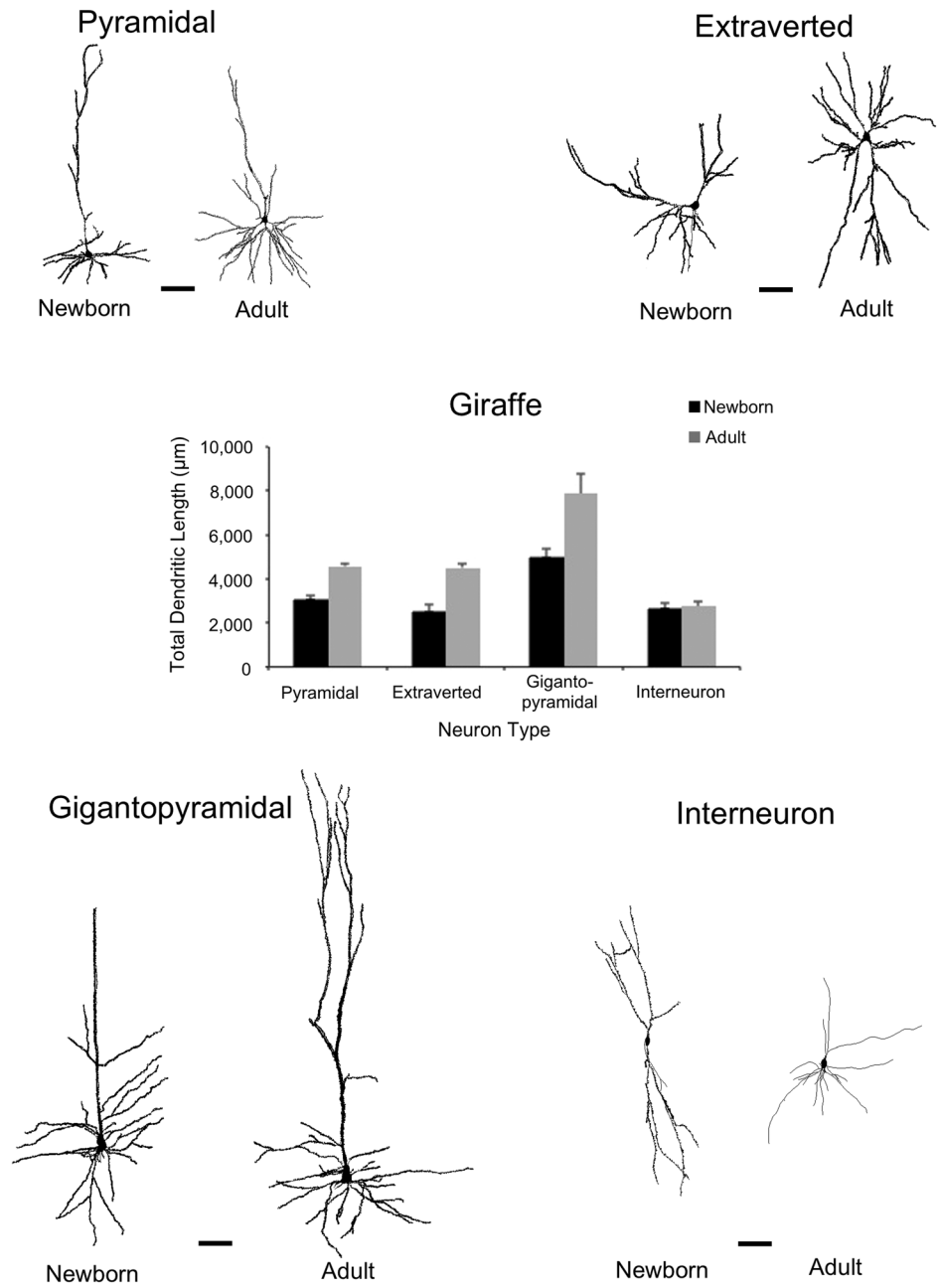

Figure 14. Bar graph of total dendritic length (TDL) of pyramidal, extraverted, gigantopyramidal, and interneurons, with representative neurolucida tracings of each neuron type from both the newborn and the adult giraffe. TDL measures were higher in the adults for all neuron types except interneurons, which exhibited similar TDL values in adults and infants. Scale bar = 100 µm.

rock hyrax, chimpanzee, dolphin, minke and humpback whale; Miller, 1988; de Lima et al., 1990; Qi et al., 1999; Sherwood et al., 2009; Butti et al., 2015). They appear to be excitatory, and constitute approximately 1–8.5% of cortical neurons, depending on the species (Mendizabal-Zubiaga et al., 2007). In the present study, these neurons were located relatively deeply in the cortex, which is expected insofar as they tend to be observed more frequently in infragranular layers (Meyer, 1987; Ferrer et al., 1986b; de Lima et al., 1990). Functionally, these atypically oriented pyramidal neurons appear to be integral components of cortical circuitry, with axons that project to ipsi- and contralateral cortical regions, as well as to the claustrum and striatum (Globus and Scheibel, 1967; Parnavelas et al., 1977; Miller, 1988; Bueno-López et al., 1991; Mendizabal-Zubiaga et al., 2007). The more horizontally oriented pyramidal neurons, in particular, appear to contribute to the lateral integration of synaptic input (Van Brederode et al., 2000).

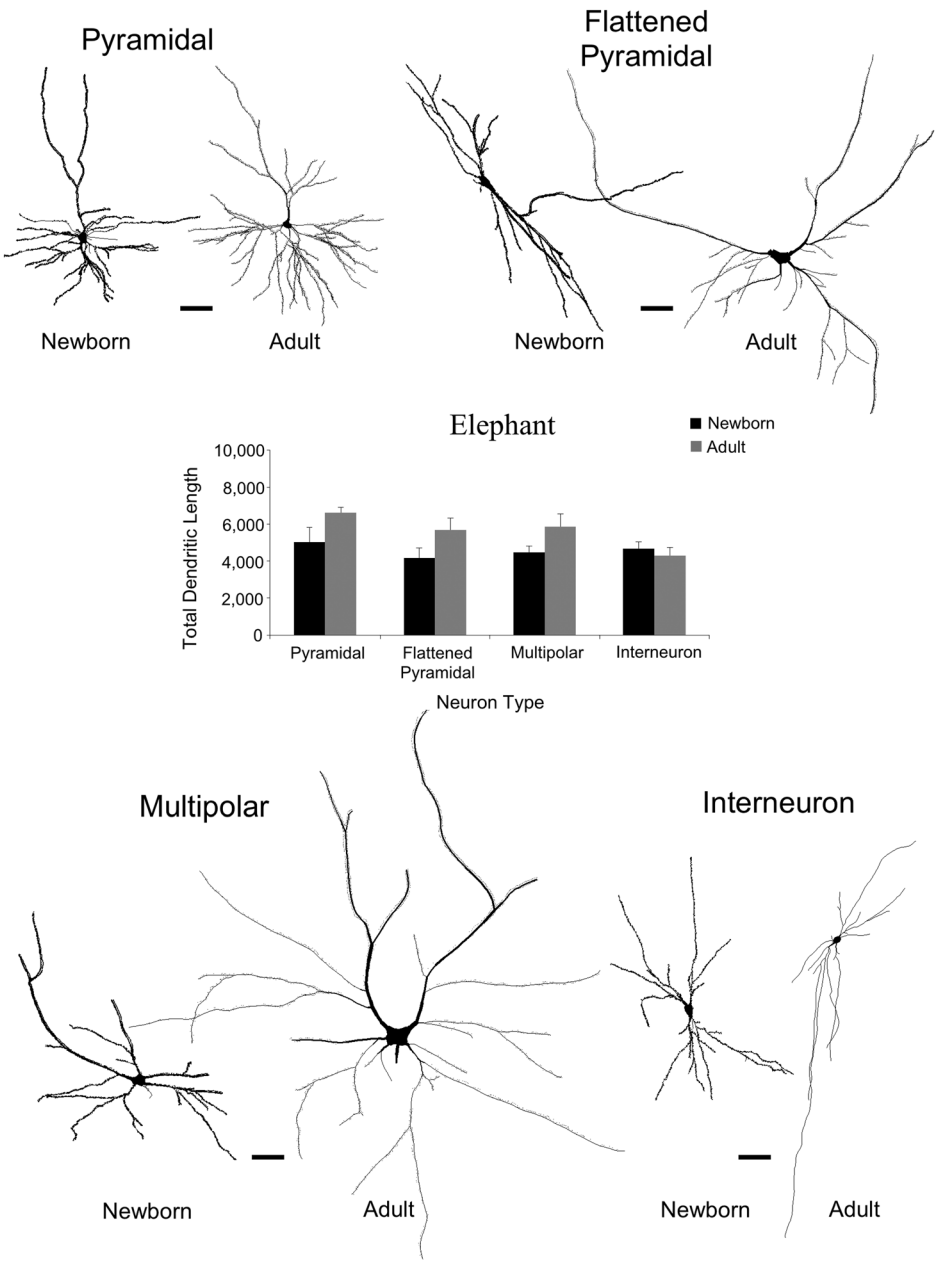

Figure 15. Bar graph of total dendritic length (TDL) of pyramidal, flattened pyramidal, nonpyramidal multipolar, and interneurons, with representative neurolucida tracings of each neuron type from both the newborn and the adult elephant. TDL measures were higher in the adults for all neuron types except interneurons, which exhibited slightly larger TDL values in the infant.Scale bar = 100 μm.

In the present study, newborn elephant cortex possessed a distinctive, clearly atypical appearance, as is salient when comparing Figures 8 and 9 in the newborn giraffe with Figures 10–12 in the newborn elephant. This unusual appearance in newborn and adult (Jacobs et al., 2011) elephant cortex is largely due to the prominent presence of three types of morphologically atypical neurons: crab-like, flattened pyramidal, and nonpyramidal multipolar (i.e., multiapical and starfish) neurons. Both the crab-like and flattened pyramidal neurons appear to be variants of neuronal morphologies that have previously been described in dog and sheep with multiple horizontal collaterals or horizontal soma shapes (Ferrer et al., 1986b). Flattened pyramidal neurons also resemble the large, widely bifurcating neurons observed by Barasa (1960) in the cow, but with a shallower, more pronounced lateral extension of the apical dendrites. The horizontal nature of these two neuronal types suggests enhanced lateral integration of information, perhaps related to the low density of elephant cortical neurons (Hart et al., 2008).

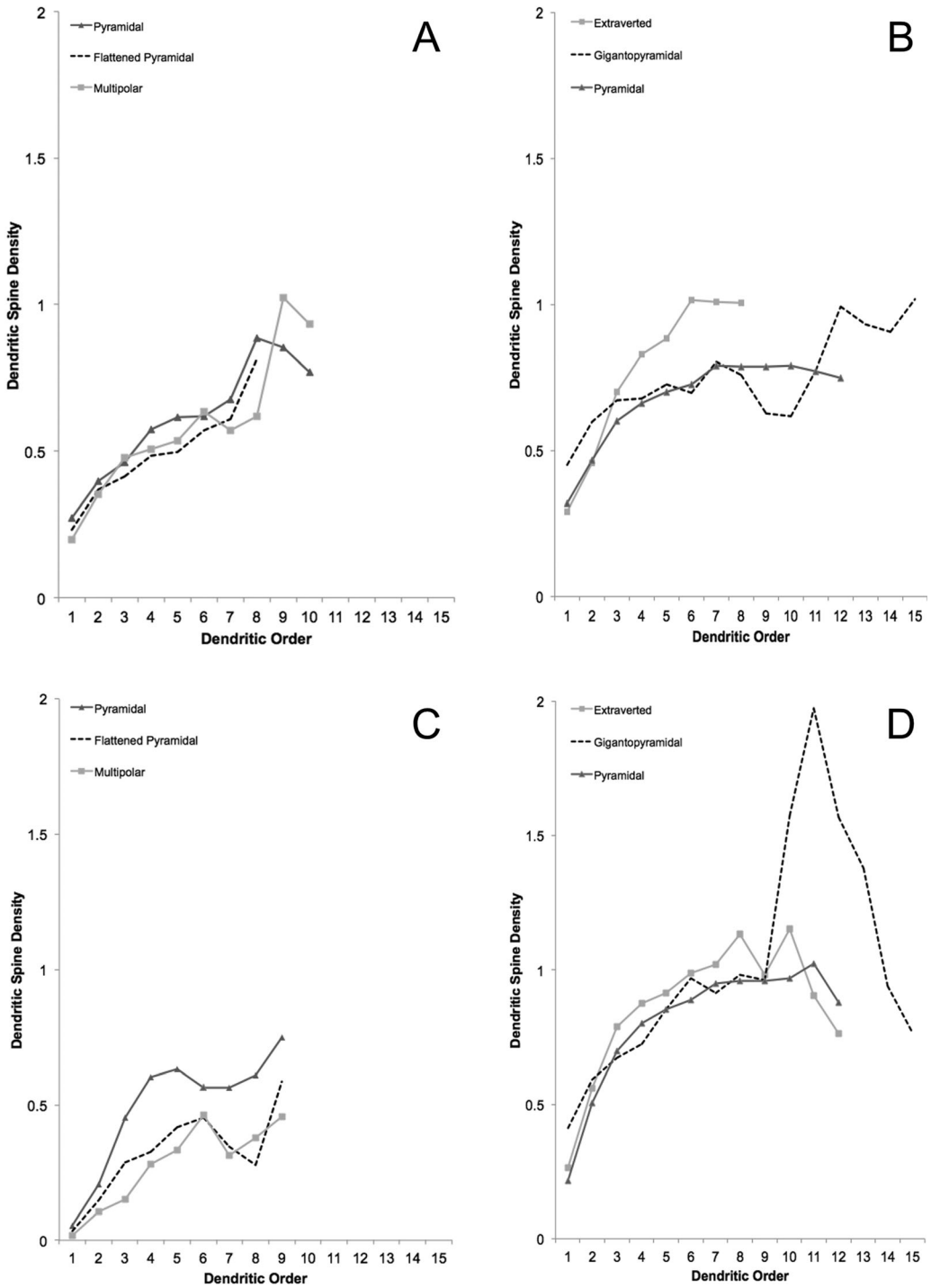

Figure 16. Envelopes for dendritic spine density (DSD) across selected neuron types in newborn elephant (**A**) and giraffe (**B**), and in adult elephant (**C**) and giraffe (**D**). These graphs indicate general somatofugal increases in DSD for all neuron types. Note that DSD values after segment order 9 in the adult giraffe (D) are clear outliers that are based on a very small number of dendritic segments. See text for details.

The most prevalent neuron type observed in the newborn elephant cortex was the nonpyramidal multipolar projection neurons, which also tended to exhibit widely bifurcating (presumably apical) dendrites. Because of the difficulty in unambiguously distinguishing apical from basilar dendrites, this type of neuron was referred to as a "multiapical pyramidal neuron" in the adult elephant (Jacobs et al., 2011). In general, neurons identified in the newborn elephant as multiapical pyramidal neurons resemble those observed in the cow, horse,

TABLE 5.

Correct–Incorrect Confusion Matrices for Differentiation of Newborn and Adult Species for Projection Neurons and Interneurons

			Predicted			Predictor importance[1]					
		93.1% Correct[2]	Adult elephant	Newborn elephant	Row total	Vol	TDL	MSL	DSC	DSN	DSD
Elephant projection neurons	Observed	Adult elephant	**21**	3	24	3	2	1	2	2	0
		Newborn elephant	1	**33**	34	Soma Size					
		Column total	22	36	58	2					
		92.0% Correct[2]	Adult giraffe	Newborn giraffe	Row total	Vol	TDL	MSL	DSC	DSN	DSD
Giraffe projection neurons	Observed	Adult giraffe	**180**	15	195	8	1	3	0	6	5
		Newborn giraffe	4	**38**	42	Soma Size					
		Column total	184	53	237	5					
		93.6% Correct[2]	Adult elephant	Newborn elephant	Row total	Vol	TDL	MSL	DSC		
Elephant interneurons	Observed	Adult elephant	**10**	1	11	1	0	1	1		
		Newborn elephant	1	**19**	20	Soma Size					
		Column total	11	20	31	1					
		70.0% Correct[b]	Adult giraffe	Newborn giraffe	Row total	Vol	TDL	MSL	DSC		
Giraffe interneurons	Observed	Adult giraffe	**16**	8	24	1	0	1	1		
		Newborn giraffe	4	**12**	16	Soma Size					
		Column total	20	20	40	0					

[1]Predictor importance indicates how many times each neuronal measure was used in the regression analysis. See text for more details.

[2]**Bold numbers** represent the correct predictions. The percentage correct is calculated by dividing the sum of the two bold numbers by the total number of neurons examined. So, for the projection neurons in elephants: $(21 + 33)/58 = 0.931$.

Abbreviations: Vol, dendritic volume; TDL, total dendritic length; DSC, dendritic segment count; MSL, mean segment length; DSN, dendritic spine number; DSD, dendritic spine density.

two-toed sloth, and anteater (Barasa, 1960; Ferrer et al., 1986b; Sherwood et al., 2009). Finally, the starfish neurons, with their five omnidirectionally radiating dendritic branches, are reminiscent of Sternzelle ("star-like" neurons) initially documented in the sei whale (Kraus and Pilleri, 1969), and subsequently in the humpback whale (Butti et al., 2015). These should not be confused with the "star pyramidal" neurons described in the rat (Lorente de Nó, 1922) or macaque monkey (Jones, 1975; Valverde, 1986) because "star pyramidal" neurons exhibit a clear, ascending apical dendrite.

Local circuit neurons

The classification of local circuit neurons was based solely on somatodendritic architecture because complete axonal arbors were not revealed in the Golgi stain, a limiting factor in the present study (Lund and Lewis, 1993; Markram et al., 2004; Druga, 2009). Nevertheless, consistent with the observation that the dendritic morphology of these neurons is rather conserved among mammals (Hof et al., 1999; Sherwood et al., 2009; DeFelipe et al., 2013), local circuit neurons in the present study appeared to exemplify several well-recognized dendritic morphologies (e.g., multipolar, bipolar, and neurogliaform), which have been identified across many species (Feldman and Peters, 1978; Jones, 1984; Ferrer et al., 1986a,b; Hassiotis et al., 2003; Thomson and Bannister, 2003; Povysheva et al., 2007; Bianchi et al., 2011), including the adult elephant (Jacobs et al., 2011) and giraffe (Butti et al., 2015). In the present sample, based on all of the neuronal measures, interneurons (i.e., multipolar and bipolar neurons) were much larger in the newborn elephant than in the newborn giraffe, although both animals exhibited higher TDL than reported by Prinz et al. (1997) for nonpyramidal neurons in human neonatal cortex. Comparison of quantitative measures across studies remains complicated, however. To this end, we examined the dendritic radius (i.e., the distance from the soma to the distal end of the longest dendrite) in both the present and previous investigations. Based on this measure, elephant interneurons are roughly the size of those observed in newborn humans (Marin-Padilla, 1969). Interneurons in both the giraffe and elephant appear to be larger than observed in the neonatal rat (Parnavelas et al., 1978; Miller, 1986), cat (Meyer and Ferres-Torres, 1984), rabbit (McMullen et al., 1988), and ferret (Peduzzi, 1988), although the dendritic extent of rodent and feline interneurons increases rapidly within the first month of life. In the present study, neurogliaform neurons were smaller than interneurons, but exhibited the same interspecies pattern, with neurogliaform neurons being larger in the newborn elephant than in the newborn giraffe. As with interneurons, neurogliaform neurons in the present sample appeared to be morphologically

similar to, but somewhat larger than, those reported in neonatal rat (Hestrin and Armstrong, 1996) and cat (Meyer and Ferres-Torres, 1984).

Two findings in the newborn elephant and giraffe differentiate local circuit neurons from the adults of these two species: 1) the presence of Cajal–Retzius neurons in the newborn elephant; and 2) the presence of dendritic spines. Although there appear to be several subtypes of layer I interneurons (Rakic and Zecevic, 2003), the term Cajal–Retzius now tends to refer to reelin-expressing (Meyer et al., 1999; Martínez-Cerdeño and Noctor, 2014) glutamatergic neurons (Ina et al., 2007), which are located in all nonolfactory cortical regions (Marin-Padilla, 1998). In the present study, Cajal–Retzius neurons resembled those described in humans (Retzius, 1893; Marin-Padilla, 1990, 2015; Meyer and González-Hernández, 1993), cats (Noback and Purpura, 1961; Meyer and Ferres-Torres, 1984), and rats (Zhou and Hablitz, 1996). In the newborn elephant, Cajal–Retzius neurons exhibited dendritic radii up to 300 μm, which is considerably larger than those observed in pre- and postnatal mice and rats (100–150 μm; Zhou and Hablitz, 1996; Meyer et al., 1998) and in humans (150–200 μm; Meyer and González-Hernández, 1993). Although the exact function of these neurons remains unclear, their morphology suggests that they constitute a convergence zone for the terminal apical dendrites of pyramidal neurons (Marin-Padilla, 1998, 2015), perhaps playing an integral role in the development of cortical circuitry (Schwartz et al., 1998; Kilb and Luhmann, 2001).

Although the presence of spines on newborn local circuit neurons has been previously documented in other species (rat: Parnavelas et al., 1978, Miller, 1986; human: Marin-Padilla, 1969), their presence in the newborn elephant and giraffe did provide these neurons with a distinctive morphological characteristic. Spines, ranging from stubby to filopodia-like protrusions (Purpura, 1975; Harris et al., 1992), were not only present on dendrites in large number, but also surrounded the somata of these neurons (Figs. 3B, 4H, 5F, 6D). The density of spines on interneurons (DSD = 0.34) in newborn giraffe and elephant is roughly equivalent to what has been documented on interneurons in rat auditory cortex between postnatal day 11 and 14 (Schachtele et al., 2011). Given that local circuit neurons in the adult giraffe (Jacobs et al., 2015) and elephant (Jacobs et al., 2011) do not exhibit such spines, their presence in the newborns of these species appears to be transitory. This loss of supernumerary spines thus appears to be a widespread developmental phenomenon in the mammalian brain beyond rodents and primates (Lund et al., 1977; Parnavelas et al., 1978; LeVay, 1973; Miller, 1986; Marrs et al., 2001).

Newborn versus adult morphology

The present findings demonstrate that newborn elephant neurons are not only larger than newborn giraffe neurons, but also that it is possible to differentiate species based on dendritic characteristics. In addition, the present findings facilitate comparison of newborn and adult neuromorphology for the giraffe and elephant because results for both time points were obtained under the same methodological conditions. For this comparison, we chose the four neuron types that were most frequently traced in the newborns and adults of each species. In the adult giraffe, a total of 204 neurons from Jacobs et al. (2015) were used: 20 interneurons, 143 pyramidal, 35 extraverted, and 6 gigantopyramidal neurons. In the adult elephant, a total of 33 neurons from Jacobs et al. (2011) were included: 11 interneurons, 16 pyramidal, 3 flattened pyramidal, and 3 nonpyramidal multipolar neurons. For newborn animals, the number of neurons is provided in Table 2. Two levels of analysis were used for this comparison.

The first, descriptive comparison examined both dendritic extent (i.e., TDL) and spine distribution (i.e., DSD) across dendritic segments. Dendritically, there was considerable morphological similarity in neuron types between newborns and adults of each species (giraffe: Fig. 14; elephant: Fig. 15), and suggested that the adult projection neurons are more dendritically extensive than the newborn counterparts. Quantitative examination of these neurons revealed that, in terms of TDL, adult projection neurons were indeed more dendritically extensive than infant projection neurons. Specifically, TDL for adult giraffe projection neurons was greater than that of their newborn counterparts by 49% for pyramidal neurons, 80% for extraverted neurons, and 59% for gigantopyramidal neurons (inset graph in Fig. 14). In elephants, TDL for adult projection neurons was greater than that of their newborn counterparts by 32% for pyramidal neurons, 36% for flattened pyramidal neurons, and 30% for nonpyramidal multipolar neurons (inset graph in Fig. 15). These results suggest a prolonged growth period for the projection neuron dendritic system, as has been documented in primates (Travis et al., 2005; Bianchi et al., 2013; Elston and Fujita, 2014). In contrast, TDL of giraffe interneurons tended to be roughly the same size (within 3%) in both the newborn and the adult (Fig. 14); TDL of elephant interneurons tended to be slightly larger (by 9%) in the infant than in the adult (Fig. 15). One explanation for the relatively large size of interneurons in the newborn is that, because of intrinsic mechanisms, these mostly γ-aminobutyric acid (GABA)-ergic interneurons may mature before the glutamatergic projection neurons

and, consequently, establish functional networks that facilitate the survival of cortical projection neurons (Köller et al., 1990; Ben-Ari, 2002; Ben-Ari et al., 2004; but see Parnavelas et al., 1978).

Using the same subset of data, a segment analysis of dendritic spines revealed a somatofugal increase in DSD for all three projection neuron types examined in the newborn elephant (Fig. 16A) and giraffe (Fig. 16B), a pattern consistent with what has been observed in human pyramidal neurons (Jacobs et al., 1997, 2001). DSD differences were small in the three neuron types examined in the newborn elephant, whereas extraverted neurons in the giraffe exhibited higher DSD after segment order 3 than either gigantopyramidal or pyramidal neurons. By comparison, DSD values in the adult elephant (Fig. 16C) were highest in pyramidal neurons. As in the newborn giraffe, DSD values in the adult giraffe were slightly higher in extraverted neurons than in the other neuron types. Note that we caution against comparison of these values across individual animals because of the small number of some neuron types and because of potential variations in tissue fixation and Golgi impregnation.

The second analysis explored these quantitative differences more completely by again using a MARSplines technique to examine potential newborn–adult differences separately for each species. As with the newborn comparisons between species, we independently examined projection neurons (elephant: pyramidal, flattened pyramidal, and multipolar neurons; giraffe: pyramidal, extraverted, and gigantopyramidal neurons) and interneurons. In other words, a conventional 2 $\times$ 2 design was used, with each comparison evaluated separately to facilitate our ability to highlight differences between the groups. The null hypothesis was that it would not be possible to differentiate either species or age group by examining the neuronal measures.

Based on the results of these analyses (Table 5), we rejected the null hypothesis of no difference between newborn and adult neurons within each species for both projection neurons [elephant: χ^2 (1) = 42.73, $P < 0.0000$; giraffe: χ^2 (1) = 136.40, $P < 0.0000$] and interneurons [elephant: χ^2 (1) = 22.88, $P < 0.0000$; giraffe: χ^2 (1) = 6.67, $P < 0.0098$]. Newborn–adult neuronal differences were above 92% accurate for all comparisons except giraffe interneurons, which were differentiated at only 70% accuracy (Table 5). In terms of predictor importance, Table 5 shows that interneurons were qualitatively weak predictors with no importance measures over 1, compared with the projection neurons importance measures of 8, 6, two 5s, two 3s, four 2s, and two 1s. Although this is a strictly qualitative result, it does indicate a considerable difference in the utility of the two classes of neurons to differentiate infants from adults. Even if one removes DSN and DSD from consideration, because those measures were not in both analyses, there is still a considerable difference in predictor importance between the two classes of neurons. This finding is consistent with the descriptive observation above, namely, that TDL measures for both species reveal very little difference in interneurons between newborns and adults. In conclusion, the MARSplines analyses reveal that, when unique combinations and weightings of the neuronal measures are considered, it is possible to discern significant differences not only between species, but also within the adults and newborns of the same species.

CONCLUSIONS

The present findings in the newborn giraffe and elephant reinforce initial observation of neocortical neuromorphology in the adults (Jacobs et al., 2011, 2015), which suggested that giraffe cortex was similar to that of other cetartiodactyls, whereas elephant cortex varied greatly from that of other eutherian mammals, including other afrotherians. Our current results show that neuronal differences between species are established in early postnatal life. Neuronal measures for both projection neurons and local circuit neurons could be used to differentiate newborn elephants from newborn giraffes, indicating fundamental species differences at the neuronal level. Finally, comparisons of neurons in newborn and adult animals indicated that projection neurons were much larger in the adults than in the newborns, whereas interneurons were roughly the same size.

ACKNOWLEDGMENTS

We thank Cheryl Stimpson for her assistance with database archiving, photo documentation, and the dissection of the newborn brains. We also thank Dr. Mark Saviano for his statistical assistance.

CONFLICT OF INTEREST STATEMENT

The authors have no conflicts of interest.

ROLE OF AUTHORS

All authors had full access to all the data in the study and take responsibility for the integrity of the data and the accuracy of the data analysis. Study concept and design: BJ, CCS, PRH. Collection of qualitative analysis of data: LL, BJ, CCS, PRH. Statistical analysis and interpretation: MS, BJ. Procurement, preparation, and fixation of tissue: AL, JJK, JFR, MAR. Obtained funding: PRH, CCS. Drafting of the manuscript: LL, BJ, MS. Photomicrography and preparation of figures: LL, BJ.

Critical revision of the manuscript for important intellectual content: MAR, JK, PAR, CCS, BJ. Study supervision: BJ, PRH, CCS.

LITERATURE CITED

Ascoli GA, Alonso-Nanclares L, Anderson SA, Barrionuevo G, Benavides-Piccione R, Burkhalter A, Buzsaki G, Cauli B, Defelipe J, Fairen A, Feldmeyer D, Fishell G, Fregnac Y, Freund TF, Gardner D, Gardner EP, Goldberg JH, Helmstaedter M, Hestrin S, Karube F, Kisvarday ZF, Lambolez B, Lewis DA, Marin O, Markram H, Munoz A, Packer A, Petersen CC, Rockland KS, Rossier J, Rudy B, Somogyi P, Staiger JF, Tamas G, Thomson AM, Toledo-Rodriguez M, Wang Y, West DC, Yuste R. 2008. Petilla terminology: nomenclature of features of GABAergic interneurons of the cerebral cortex. Nat Rev Neurosci 9: 557–568.

Badlangana NL, Bhagwandin A, Fuxe K, Manger PR. 2007. Observations on the giraffe central nervous system related to the corticospinal tract, motor cortex and spinal cord: what difference does a long neck make? Neuroscience 148:522–534.

Barasa A. 1960. Forma, grandezza e densitá dei neuroni della corteccia cerebrale in mammiferi di grandezza corporea differente. Z Zellforsch 53:69–89.

Becker LE, Armstrong DL, Chan F, Wood MM. 1984. Dendritic development in human occipital cortical neurons. Dev Brain Res 13:117–124.

Ben-Ari Y. 2002. Excitatory actions of GABA during development: the nature of the nurture. Nat Rev Neurosci 3: 728–739.

Ben-Ari Y, Khalilov I, Represa A, Gozlan H. 2004. Interneurons set the tune of developing networks. Trends Neurosci 27:422–427.

Berk RA, Freedman DA. 2003. Statistical assumptions as empirical commitments. In: Cohen S, Blomberg TG, eds. Punishment and social control: essays in honor of Sheldon L. Messinger. New Brunswick: Aldine de Gruyter. p 235–254.

Betz W. 1874. Anatomischer Nachweis zweier Gehirncentra. Zentralbl Med Wiss 12:578–580, 595–599.

Bianchi S, Bauernfeind AL, Gupta K, Stimpson CD, Spocter MA, Bonar CJ, Manger PR, Hof PR. Jacobs B, Sherwood CC. 2011. Neocortical neuron morphology in Afrotheria: comparing the rock hyrax with the African elephant. Ann N Y Acad Sci 1225:37–46.

Bianchi S, Stimpson CD, Bauernfeind AL, Schapiro SJ, Baze WB, McArthur MJ, Bronson E, Hopkins WD, Semendeferi K, Jacobs B, Hof PR, Sherwood CC. 2012. Dendritic morphology of pyramidal neurons in the chimpanzee neocortex: regional specializations and comparison to humans. Cereb Cortex 23:429–2436.

Bianchi S, Stimpson CD, Duka T, Larsen MD, Janssen WG, Collins Z, Bauernfeind AL, Schapiro SJ, Baze WB, McArthur MJ, Hopkins WD, Wildman DE, Lipovich L, Kuzawa CW, Jacobs B, Hof PR, Sherwood CC. 2013. Synaptogenesis and development of pyramidal neuron dendritic morphology in the chimpanzee neocortex. Proc Natl Acad Sci U S A 110(suppl 2):10395–10401.

Bock J, Gruss M, Becker S, Braun K. 2005. Experience-induced changes of dendritic spine densities in the prefrontal and sensory cortex: correlation with developmental time windows. Cereb Cortex 15:802–808.

Bok ST. 1959. Histonomy of the cerebral cortex. Amsterdam: Elsevier.

Bota MB, Swanson LW. 2007. The neuron classification problem. Brain Res Rev 56:79–88.

Braak H, Braak E. 1985. Golgi preparations as a tool in neuropathology with particular reference to investigations of the human telencephalic cortex. Prog Neurobiol 25:93–139.

Bueno-López JL, Reblet C, López-Medina A, Gómez-Urquijo, Grandes P, Gondra J, Hennequet L. 1991. Targets and laminar distribution of projection neurons with "inverted" morphology in rabbit cortex. Eur J Neurosci 3:415–430.

Butti C, Fordyce ER, Raghanti MA, Gu X, Bonar CJ, Wicinski BA, Wong EW, Roman J, Brake A, Eaves E, Spocter MA, Tang CY, Jacobs B, Sherwood CC, Hof PR. 2014. The cerebral cortex of the pygmy hippopotamus, *Hexaprotodon liberiensis* (Cetartiodactyla, Hippopotamidae): MRI, cytoarchitecture, and neuronal morphology. Anat Rec 297:670–700.

Butti C, Janeway CM, Townshend C, Ridgway SH, Manger PR, Sherwood CC, Hof PR, Jacobs B. 2015. Neuronal morphology in cetartiodactyls. I. A comparative Golgi analysis of neuronal morphology in the bottlenose dolphin (*Tursiops truncatus*), the minke whale (*Balaenoptera acutorostrata*), and the humpback whale (*Megaptera novaeangliae*). Brain Struct Funct, in press. doi: 10.1007/s00429-014-0860-3.

DeFelipe J, López-Cruz PL, Benavides-Piccione R, Bielza C, Larrañaga P, Anderson S, Burkhalter A, Cauli B, Fairén A, Feldmeyer D, Fishell G, Fitzpatrick D, Freund TF, González-Burgos G, Hestrin S, Hill S, Hof PR, Huang J, Jones EG, Kawaguchi Y, Kisvárday Z, Kubota Y, Lewis DA, Marín O, Markram H, McBain CJ, Meyer HS, Monyer H, Nelson SB, Rockland K, Rossier J, Rubenstein JLR, Rudy B, Scanziani M, Shepherd GM, Sherwood CC, Staiger JF, Tamás G, Thomson A, Wang Y, Yuste R, Ascoli GA. 2013. New insights into the classification and nomenclature of cortical GABAergic interneurons. Nat Rev Neurosci 14:202–216.

de Lima AD, Voigt T, Morrison JH. 1990. Morphology of the cells within the inferior temporal gyrus that project to the prefrontal cortex in the macaque monkey. J Comp Neurol 296:159–172.

Druga R. 2009. Neocortical inhibitory system. Folia Biol 55: 201–217.

Elston GN, Fujita I. 2014. Pyramidal cell development: postnatal spinogenesis, dendritic growth, axon growth, and electrophysiology. Front Neuroanat 8:78.

Feldman ML, Peters A. 1978. The forms of non-pyramidal neurons in the visual cortex of the rat. J Comp Neurol 179: 761–793.

Ferrer I, Perera M. 1988. Structure and nerve cell organisation in the cerebral cortex of the dolphin *Stenella coeruleoalba* a Golgi study: with special attention to the primary auditory area. Anat Embryol (Berl) 178:161–173.

Ferrer I, Fábrigues I, Condom E. 1986a. A Golgi study of the sixth layer of the cerebral cortex I. The lissencephalic brain of Rodentia, Lagomorpha, Insectivora and Chiroptera. J Anat 145:217–234.

Ferrer I, Fábrigues I, Condom E. 1986b. A Golgi study of the sixth layer of the cerebral cortex II. The gyrencephalic brain of Carnivora, Artiodactyla and primates. J Anat 146:87–104.

Fitzpatrick DC, Henson OW Jr. 1994. Cell types in the mustached bat auditory cortex. Brain Behav Evol 43:79–91.

Fleischhauer K, Petsche H, Wittkowski W. 1972. Vertical bundles of dendrites in the neocortex. Anat Embryol 136: 213–223.

Friedman JH. 1991. Multivariate adaptive regression splines. Ann Stat 19:1–67.

Germroth P, Schwerdtfeger WK, Buhl EH. 1989. Morphology of identified entorhinal neurons projecting to the

hippocampus. A light microscopical study combining retrograde tracing and intracellular injection. Neuroscience 30:683–691.

Glezer II, Morgane PJ. 1990. Ultrastructure of synapses and Golgi analysis of neurons in neocortex of the lateral gyrus (visual cortex) of the dolphin and pilot whale. Brain Res Bull 24:401–427.

Globus A, Scheibel AB. 1967. Pattern and field in cortical structure: the rabbit. J Comp Neurol 131:155–172.

Hall-Martin AJ, Skinner JD, Hopkins BJ. 1978. The development of the reproductive organs of the male giraffe, *Giraffa camelopardalis*. J Reprod Fertil 52:1–7.

Harris KM, Jensen FE, Tsao B. 1992. Three-dimensional structure of dendritic spines and synapses in rat hippocampus (CA1) at postnatal day 15 and adult ages: implications for the maturation of synaptic physiology and long-term potentiation. J Neurosci 12:2685–2705.

Hart BL, Hart LA, Pinter-Wollman N. 2008. Large brains and cognition: where do elephants fit in? Neurosci Biobehav Rev 32:86–98.

Hassiotis M, Paxinos G, Ashwell KWS. 2003. The anatomy of the cerebral cortex of the echidna (*Tachyglossus aculeatus*). Comp Biochem Physiol A 136:827–850.

Hastie T, Tibshirani R, Friedman J. 2009. The elements of statistical learning, 2nd ed. New York: Springer.

Hestrin S, Armstrong WE. 1996. Morphology and physiology of cortical neurons in layer I. J Neurosci 16:5290–5300.

Hof PR, Glezer II, Condé F, Flagg RA, Rubin MB, Nimchinsky EA, Vogt Weisenhorn DM. 1999. Cellular distribution of the calcium-binding proteins parvalbumin, calbindin, and calretinin in the neocortex of mammals: phylogenetic and developmental patterns. J Chem Neuroanat 16:77–116.

Hof PR, Van der Gucht E. 2007. Structure of the cerebral cortex of the humpback whale, *Megaptera novaeangliae* (Cetacea, Mysticeti, Balaeopteridae). Anat Rec 290:1–31.

Horner CH, Arbuthnott E. 1991. Methods of estimation of spine density—are spines evenly distributed throughout the dendritic field? J Anat 177:179–184.

Ina A, Sugiyama M, Konno J, Yoshida S, Ohmomo H, Nogami H, Shutoh F, Hisano S. 2007. Cajal–Retzius cells and subplate neurons differentially express vesicular glutamate transporters 1 and 2 during development of mouse cortex. Eur J Neurosci 26:615–623.

Innocenti GM, Vercelli A. 2010. Dendritic bundles, minicolumns, columns, and cortical output units. Front Neuroanat 4:11.

Jacobs B, Driscoll L, Schall M. 1997. Life-span dendritic and spine changes in areas 10 and 18 of human cortex: a quantitative Golgi study. J Comp Neurol 386:661–680.

Jacobs B, Harland T, Kennedy D, Schall M, Wicinski B., Butti C, Hof PR, Sherwood CC, Manger PR. 2015. The neocortex of cetartiodactyls. II. Neuronal morphology of the visual and motor cortices in the giraffe (*Giraffa camelopardalis*). Brain Struct Funct, in press doi: 10.1007/s00429–014–0830–9.

Jacobs B, Johnson N, Wahl D, Schall M, Maseko BC, Lewandowski A, Raghanti MA, Wicinski B, Butti C, Hopkins WD, Bertelsen MF, Reep RL, Hof PR, Sherwood CC, Manger PR. 2014. Comparative neuronal morphology of cerebellar cortex in afrotherians (African elephant, Florida manatee), primates (human, common chimpanzee), cetartiodactyls (humpback whale, giraffe), and carnivores (Siberian tiger, clouded leopard). Front Neuroanat 8:24.

Jacobs B, Lubs J, Hannan M, Anderson K, Butti C, Sherwood CC, Hof PR, Manger PR. 2011. Neuronal morphology in the African elephant (*Loxodonta africana)* neocortex. Brain Struct Funct 215:273–298.

Jacobs B, Schall M, Prather M, Kapler E, Driscoll L, Baca S. 2001. Regional dendritic and spine variation in human cerebral cortex: a quantitative Golgi study. Cereb Cortex 11:558–571.

Jacobs B, Scheibel AB. 1993. A quantitative dendritic analysis of Wernicke's area in humans. I. Lifespan changes. J Comp Neurol 327:83–96.

Jacobs B, Scheibel AB. 2002. Regional dendritic variation in primate cortical pyramidal cells. In: Schüz A, Miller R, eds. Cortical areas: unity and diversity (Conceptual Advances in Brain Research Series). London: Taylor & Francis. p 111–131.

Jones EG. 1975. Varieties and distribution of non-pyramidal cells in the somatic sensory cortex of the squirrel monkey. J Comp Neurol 160:205–268.

Jones EG. 1984. Neurogliaform or spiderweb cells. In: Peters A, Jones EG, eds. Cerebral cortex. New York: Plenum Press. p 409–418.

Kilb W, Luhmann HJ. 2001. Spontaneous GABAergic postsynaptic currents in Cajal-Retzius cells in neonatal rat cerebral cortex. Eur J Neurosci 13:1387–1390.

Köller H, Siebler M, Schmalenbach C, Müller H-W. 1990. GABA and glutamate receptor development of cultured neurons from rat hippocampus, septal region, and neocortex. Synapse 5:59–64.

Kraus C, Pilleri G. 1969. Zur Histologie der Grosshirnrinde von *Balaenoptera borealis* (Cetacea, Mysticeti). Invest Cetacea 1:151–170.

Landrieu P, Goffinet A. 1981. Inverted pyramidal neurons and their axons in the neocortex of the reeler mutant mice. Cell Tissue Res 218:293–301.

LeVay S. 1973. Synaptic patterns in the visual cortex of the cat and monkey. Electron microscopy of Golgi preparations. J Comp Neurol 150:53–86.

Lorente de Nó R. 1922. La corteza cerebral del ratón. Primera contribución. La corteza acústica. Trab Lab Invest Biol Univ Madrid 20:41–78.

Lu D, He L, Xiang W, Ai W-M, Cao Y, Wang X-S, Pan A, Luo X-G, Li Z, Yan X-X. 2013. Somal and dendritic development of human CA3 pyramidal neurons from midgestation to middle childhood: a quantitative Golgi study. Anat Rec 296:123–132.

Lund JS, Lewis DA. 1993. Local circuit neurons of developing and mature macaque prefrontal cortex: Golgi and immunocytochemical characteristics. J Comp Neurol 328:282–312.

Lund JS, Boothe RG, Lund RD. 1977. Development of neurons in the visual cortex (area 17) of the monkey (*Macaca nemestrina*): a Golgi study from fetal day 127 to postnatal maturity. J Comp Neurol 176:149–187.

Manger PR, Cort J, Ebrahim N, Goodman A, Henning J, Karolia M, Rodrigues S-L, Strkalj G. 2008. Is 21st century neuroscience too focused on the rat/mouse model of the brain function and dysfunction? Front Neuroanat 2:5.

Marin-Padilla M. 1969. Origin of the pericellular baskets of the pyramidal cells of the human motor cortex: a Golgi study. Brain Res 14:633–646.

Marin-Padilla M. 1971. Early prenatal ontogenesis of the cerebral cortex (neocortex) of the cat (*Felis domestica*). A Golgi study. Z Anat Entwickl-Gesch 134:117–145.

Marin-Padilla M. 1972. Prenatal ontogenetic history of the principal neurons of the neocortex of the cat (*Felis domestica*). A Golgi study. II. Developmental differences and their significances. Z Anat Entwickl-Gesch 136:125–142.

Marin-Padilla M. 1990. Three-dimensional structural organization of layer I of the human cerebral cortex: a Golgi study. J Comp Neurol 299:89–105.
Marin-Padilla M. 1992. Ontogenesis of the pyramidal cell of the mammalian neocortex and developmental cytoarchitectonics: a unifying theory. J Comp Neurol 321:223–240.
Marin-Padilla M. 1998. Cajal-Retzius cells and the development of the neocortex. Trends Neurosci 21:64–71.
Marin-Padilla M. 2014. The mammalian neocortex new pyramidal neuron: a new conception. Front Neuroanat 5:51.
Marin-Padilla M. 2015. Human cerebral cortex Cajal-Retzius neuron: development, structure and function. A Golgi study. Front Neuroanat 9:21.
Markram H, Toledo-Rodriguez M, Wang Y, Gupta A, Silberberg G, Wu C. 2004. Interneurons of the neocortical inhibitory system. Nat Rev Neurosci 5:793–807.
Marrs GS, Green SH, Dailey ME. 2001. Rapid formation and remodeling of postsynaptic densities in developing dendrites. Nat Neurosci 4:1006–1013.
Martínez-Cerdeño V, Noctor SC. 2014. Cajal, Retzius, and Cajal-Retzius cells. Front Neuroanat 8:48.
Masland RH. 2004. Neuronal cell types. Curr Biol 14:R497–R500.
McMullen NT, Goldberger B, Glaser EM. 1988. Postnatal development of lamina III/IV nonpyramidal neurons in rabbit auditory cortex: quantitative and spatial analyses of Golgi-impregnated material. J Comp Neurol 278:139–155.
Mendizabal-Zubiaga JL, Reblet C, Bueno-Lopez JL. 2007. The underside of the cerebral cortex: layer V/VI spiny inverted neurons. J Anat 211:223–236.
Meyer G. 1987. Forms and spatial arrangement of neurons in the primary motor cortex of man. J Comp Neurol 262: 402–428.
Meyer G, Ferres-Torres R. 1984. Postnatal maturation of nonpyramidal neurons in the visual cortex of the cat. J Comp Neurol 228:226–244.
Meyer G, González-Hernández T. 1993. Developmental changes in layer I of the human neocortex during prenatal life: a DiI-tracing and AChE and NADPH-d histochemistry study. J Comp Neurol 338:317–336.
Meyer G, Soria JM, Martínez-Galán JR, Martín-Clemente B, Fairén A. 1998. Different origins and developmental histories of transient neurons in the marginal zone of the fetal and neonatal rat cortex. J Comp Neurol 397:493–518.
Meyer G, Goffinet AM, Fairén A. 1999. What is a Cajal-Retzius cell? A reassessment of a classical cell type based on recent observations in the developing neocortex. Cereb Cortex 9:765–775.
Millar JS, Zammuto RM. 1983. Life histories of mammals: an analysis of life tables. Ecology 64:631–635.
Miller MW. 1981. Maturation of rat visual cortex. I. A quantitative study of Golgi-impregnated pyramidal neurons. J Neurocytol 10:859–878.
Miller MW. 1986. Maturation of rat visual cortex. III. Postnatal morphogenesis and synaptogenesis of local circuit neurons. Brain Res 25:271–285.
Miller MW. 1988. Maturation of rat visual cortex: IV. The generation, migration, morphogenesis, and connectivity of atypically oriented pyramidal neurons. J Comp Neurol 274:387–405.
Mitchell G, Bobbitt JP, Devries S. 2008. Cerebral perfusion pressure in giraffe: modeling the effects of head-raising and -lowering. J Theor Biol 252:98–108.
Molnár Z, Cheung AFP. 2006. Towards the classification of subpopulations of layer V pyramidal projection neurons. Neurosci Res 55:105–115.
Moss CJ, Lee PC. 2011. Female reproductive strategies: individual life histories. In: Moss CJ, Croze H, Lee PC, eds. The Amboseli elephants. Chicago: University of Chicago Press. p 187–204.
Mountcastle VB. 1997. The columnar organization of the neocortex. Brain 120:701–722.
Murmu MS, Salomon S, Biala Y, Weinstock M, Braun K, Bock J. 2006. Changes of spine density and dendritic complexity in the prefrontal cortex in offspring of mothers exposed to stress during pregnancy. Eur J Neurosci 24: 1477–1487.
Nelson SB, Sugino K, Hempel CM. 2006. The problem of neuronal cell types: a physiological genomics approach. Trends Neurosci 29:339–345.
Noback CR, Purpura DP. 1961. Postnatal ontogenesis of neurons in cat neocortex. J Comp Neurol 117:291–307.
Parnavelas JG, Lieberman AR, Webster KE. 1977. Organization of neurons in the visual cortex, area 17, of the rat. J Anat 124:305–322.
Parnavelas JG, Bradford R, Mounty EJ, Lieberman AR. 1978. The development of non-pyramidal neurons in the visual cortex of the rat. Anat Embryol 155:1–14.
Peduzzi JD. 1988. Genesis of GABA-immunoreactive neurons in the ferret visual cortex. J Neurosci 8:920–931.
Petanjek Z, Judaš M, Kostović I, Uylings BM. 2008. Lifespan alterations of basal dendritic trees of pyramidal neurons in the human prefrontal cortex: a layer-specific pattern. Cereb Cortex 18:915–929.
Povysheva NY, Zaitsev AV, Kröner S, Krimer OA, Rotaru DC, González-Burgos G, Lewis DA, Krimer LS. 2007. Electrophysiological differences between neurogliaform cells from monkey and rat prefrontal cortex. J Neurophysiol 97:1030–1039.
Prinz M, Prinz B, Schulz E. 1997. The growth of non-pyramidal neurons in the primary motor cortex of man: a Golgi study. Histol Histopathol 12:895–900.
Purpura DP. 1975. Dendritic differentiation in human cerebral cortex: normal and aberrant developmental patterns. Adv Neurol 12:91–134.
Qi H-X, Jain N, Preuss TM, Kaas JH. 1999. Inverted pyramidal neurons in chimpanzee sensorimotor cortex are revealed by immunostaining with monoclonal antibody SMI-32. Somatosens Mot Res 16:49–56.
Rakic S, Zecevic N. 2003. Emerging complexity of layer I in human cerebral cortex. Cereb Cortex 13:1072–1083.
Ramón y Cajal S. 1891. Sur la structure de l'écorce cérébrale de quelques mammifères. La Cellule 7:123–176. English translation in DeFelipe J, Jones EG. 1988. Cajal on the cerebral cortex. Oxford: Oxford University Press. p 23–54.
Retzius G. 1893. Die Cajal'schen Zellen der Grosshirnrinde beim Menschen und bei Säugetieren. Biol Untersuch Neue Folge 5:1–8.
Roitman MF, Na E, Anderson G, Jones TA, Bernstein IL. 2002. Induction of a salt appetite alters dendritic morphology in nucleus accumbens and sensitizes rats to amphetamine. J Neurosci 22:RC225.
Sacher GA, Staffeldt EF. 1974. Relation of gestation time to brain weight for placental mammals: implications for the theory of vertebrate growth. Am Nat 108:593–615.
Sanides F, Sanides D. 1972. The "extraverted neurons" of the mammalian cerebral cortex. Z Anat Entwickl-Gesch 136: 272–293.
Schachtele SJ, Losh J, Dailey ME, Green SH. 2011. Spine formation and maturation in the developing rat auditory cortex. J Comp Neurol 519:3327–3345.
Schadé JP, Caveness WF. 1968. IV. Alteration in dendritic organization. Brain Res 7:59–86.

Scheibel ME, Davies TL, Lindsay RD, Scheibel AB. 1974. Basilar dendrite bundles of giant pyramidal cells. Exp Neurol 42:307–319.

Scheibel ME, Scheibel AB. 1978a. The dendritic structure of the human Betz cell. In: Brazier MAB, Pets H, eds. Architectonics of the cerebral cortex. New York: Raven Press. p 43–57.

Scheibel ME, Scheibel AB. 1978b. The methods of Golgi. In: Robertson RT, ed. Neuroanatomical research techniques. New York: Academic Press. p 89–114.

Schwartz TH, Rabinowitz D, Unni V, Kumar VS, Smetters DK, Tsiola A, Yuste R. 1998. Networks of coactive neurons in developing layer 1. Neuron 20:541–552.

Sherwood CC, Stimpson CD, Butti C, Bonar CJ, Newton AL, Allman JM, Hof PR. 2009. Neocortical neuron types in Xenarthra and Afrotheria: implications for brain evolution in mammals. Brain Struct Funct 213:301–328.

Sholl DA. 1953. Dendritic organization of the neurons of the visual and motor cortices of the cat. J Anat 87:387–406.

Shoshani J, Kupsky WJ, Marchant GH. 2006. Elephant brain part I: Gross morphology, functions, comparative anatomy, and evolution. Brain Res Bull 70:124–157.

Simat M, Parpan F, Fritschy J-M. 2007. Heterogeneity of glycinergic and GABAergic interneurons in the granule cell layer of mouse cerebellum. J Comp Neurol 500:71–83.

Takashima S, Becker LE, Armstrong DL, Chan F. 1981. Abnormal neuronal development in the visual cortex of the human fetus and infant with Down's syndrome. A quantitative and qualitative Golgi study. Brain Res 225:1–21.

Thomson AM, Bannister AP. 2003. Interlaminar connections in the neocortex. Cereb Cortex 13:5–15.

Travis K, Ford K, Jacobs B. 2005. Regional dendritic variation in neonatal human cortex: a quantitative Golgi study. Dev Neurosci 27: 277–287.

Uylings HBM, Ruiz-Marcos A, van Pelt J. 1986. The metric analysis of three-dimensional dendritic tree patterns: a methodological review. J Neurosci Methods 18:127–151.

Valverde F. 1986. Intrinsic neocortical organization: some comparative aspects. Neuroscience 18:1–23.

Van der Loos H. 1965. The "improperly" oriented pyramidal cell in the cerebral cortex and its possible bearing on problems of neuronal growth and cell orientation. Bull Johns Hopkins Hosp 117:228–250.

Van Brederode JFM, Foehring RC, Spain WJ. 2000. Morphological and electrophysiological properties of atypically oriented layer 2 pyramidal cells of the juvenile rat neocortex. Neuroscience 101:851–861.

Williams RS, Ferrante RJ, Caviness VS Jr. 1978. The Golgi rapid method in clinical neuropathology: the morphologic consequences of suboptimal fixation. J Neuropathol Exp Neurol 37:13–33.

Zhou F, Hablitz JJ. 1996. Morphological properties of intracellularly labeled layer I neurons in rat neocortex. J Comp Neurol 376:198–213.